

SANDIA REPORT

SAND96-2090 • UC-903
Unlimited Release
Printed August 1996

RECEIVED

AUG 30 1996

OSTI

Unsaturated Hydrologic Flow Parameters Based on Laboratory and Field Data For Soils Near the Mixed Waste Landfill, Technical Area III, Sandia National Laboratories/New Mexico

Craig S. Roepke, Warren R. Strong, Huy A. Nguyen, Michael D. McVey, Timothy J. Goering

Prepared by
Sandia National Laboratories
Albuquerque, New Mexico 87185 and Livermore, California 94550
for the United States Department of Energy
under Contract DE-AC04-94AL85000

Approved for public release; distribution is unlimited.



SF2900Q(8-81)

DISTRIBUTION OF THIS DOCUMENT IS UNLIMITED

lm

MASTER

Issued by Sandia National Laboratories, operated for the United States Department of Energy by Sandia Corporation.

NOTICE: This report was prepared as an account of work sponsored by an agency of the United States Government. Neither the United States Government nor any agency thereof, nor any of their employees, nor any of their contractors, subcontractors, or their employees, makes any warranty, express or implied, or assumes any legal liability or responsibility for the accuracy, completeness, or usefulness of any information, apparatus, product, or process disclosed, or represents that its use would not infringe privately owned rights. Reference herein to any specific commercial product, process, or service by trade name, trademark, manufacturer, or otherwise, does not necessarily constitute or imply its endorsement, recommendation, or favoring by the United States Government, any agency thereof or any of their contractors or subcontractors. The views and opinions expressed herein do not necessarily state or reflect those of the United States Government, any agency thereof or any of their contractors.

Printed in the United States of America. This report has been reproduced directly from the best available copy.

Available to DOE and DOE contractors from
Office of Scientific and Technical Information
PO Box 62
Oak Ridge, TN 37831

Prices available from (615) 576-8401, FTS 626-8401

Available to the public from
National Technical Information Service
US Department of Commerce
5285 Port Royal Rd
Springfield, VA 22161

NTIS price codes
Printed copy: A03
Microfiche copy: A01

SAND96-2090
Unlimited Release
Printed August 1996

Distribution
Category UC-903

**Unsaturated Hydrologic Flow Parameters Based on
Laboratory and Field Data For Soils Near the Mixed Waste Landfill,
Technical Area III, Sandia National Laboratories/New Mexico**

Craig S. Roepke
INTERA, Inc.
1650 University Boulevard,
Albuquerque, NM 87102

Warren R. Strong and Huy A. Nguyen
Environmental Restoration Project
Sandia National Laboratories
Albuquerque, NM 87185

Michael D. McVey and Timothy J. Goering
GRAM, Inc.
8500 Menaul Blvd., NE, Suite B-370
Albuquerque, NM 87112

Abstract

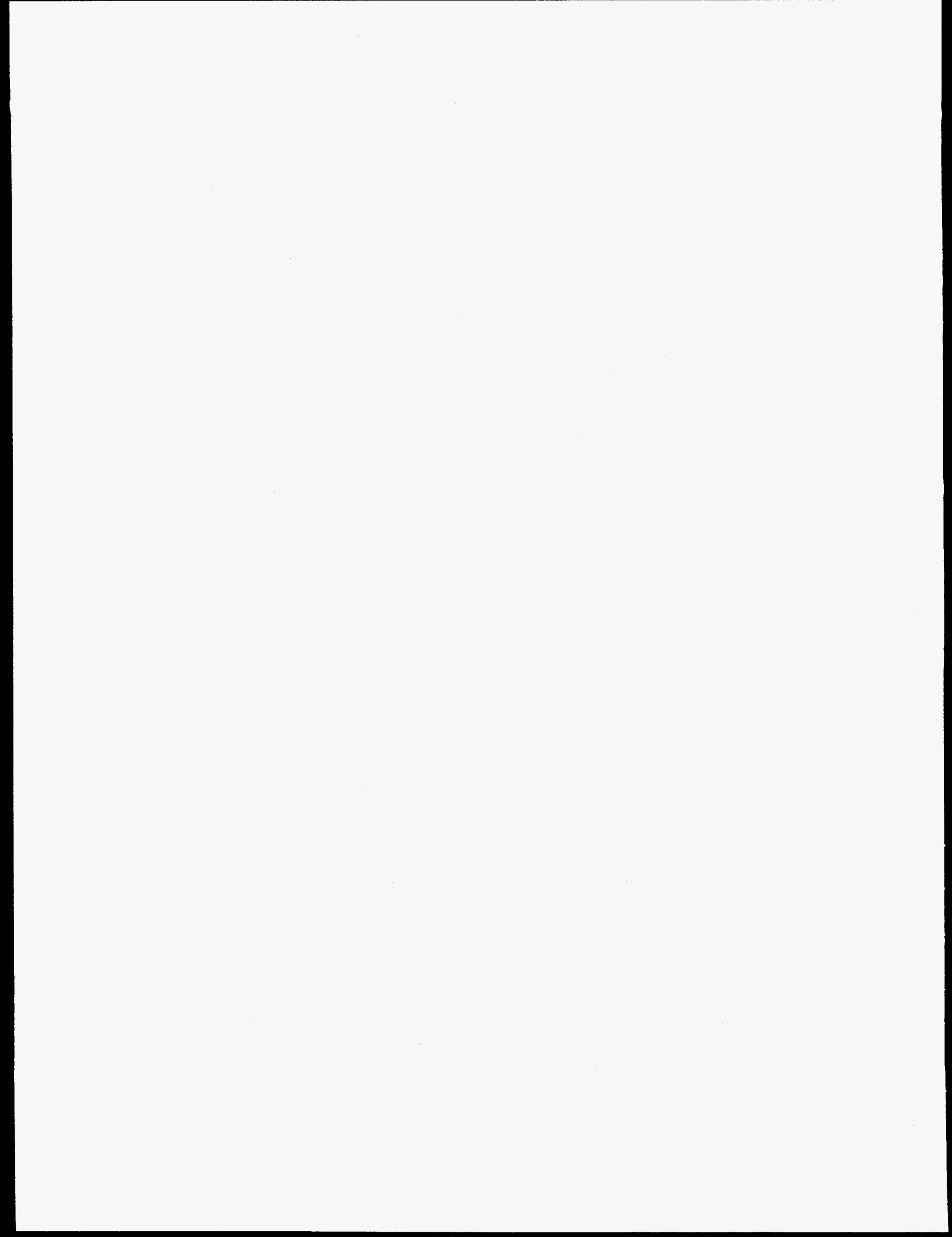
This report presents the results of laboratory tests conducted on soil core samples obtained prior to an instantaneous profile test conducted west of the Mixed Waste Landfill in Technical Area III. The instantaneous profile test was conducted to measure *in situ* hydrologic parameters controlling unsaturated flow and contaminant transport in the near-surface vadose zone. Soil core samples from the instantaneous profile test plot were tested in the Sandia National Laboratory's Environmental Restoration Project Hydrology Laboratory to measure saturated hydraulic conductivity and the relationships between moisture content and soil water tension. Data from laboratory tests and the instantaneous profile field test were then modeled using the computer code RETC to quantify moisture content, soil water tension, and unsaturated hydraulic conductivity relationships. Results verified that a combination of laboratory and field data yielded a more complete definition of hydrologic properties than either laboratory or field data alone. Results also indicated that at native moisture contents, the potential for significant unsaturated aqueous flow is limited, while at saturated or near-saturated conditions, preferential flow may occur.

Acknowledgments

The authors wish to thank Jerry Peace (Dept. 7585) for his sponsorship of this project. The authors also wish to acknowledge Randy Roberts (CDM-Federal Programs Center) and Monica Archuleta (CDM-Federal Programs Center) for conducting the laboratory operations so critical to the success of this study.

DISCLAIMER

**Portions of this document may be illegible
in electronic image products. Images are
produced from the best available original
document.**



Contents

1.0 Introduction	1
2.0 The MWL IP Test	2
2.1 IP Test Description.....	2
2.2 Sample Locations.....	2
2.3 Sample Preparation and testing.....	2
3.0 Results	3
3.1 Fitting of van Genuchten Parameters and Modeling of $K(\theta)$ Relationships	3
3.2 Saturated Hydraulic Conductivity Predicted by RETC Modeling	4
3.3 Unsaturated Hydraulic Conductivity	5
4.0 Conclusions	5
5.0 References	7
APPENDIX A: RETC Predictions of $\psi(\theta)$ and $K(\theta)$ Relationships for Soils in the Vadose Zone Near the Mixed Waste Landfill ..	A-1

Tables

1 RETC-derived parameters from
 $\psi(\theta)$ data of laboratory-tested samples..... 8

2 RETC-derived parameters from *in situ*
 K(θ) data derived during the IP test..... 9

3 RETC-derived parameters from combined
 laboratory $\psi(\theta)$ and *in situ* K(θ) data..... 9

Figures

1 Instantaneous profile test plot location..... 10

2 Instrument locations in the IP test plot..... 11

3 Saturated hydraulic conductivity with depth..... 12

4 RETC-predicted hydraulic conductivity-moisture content relationships
 based on field, laboratory, and combined field and laboratory data..... 13

5 RETC predictions of saturated moisture content
 based on laboratory testing 14

6 Hydraulic conductivity with depth at a volumetric
 moisture content of 10 percent..... 15

Nomenclature

bgs	below ground surface
cm	centimeter
ER	Environmental Restoration
IP	instantaneous profile
K_s	saturated hydraulic conductivity [L/T]
K_{eff}	effective hydraulic conductivity [L/T]
$K(\theta)$	unsaturated hydraulic conductivity as a function of volumetric moisture content [L/T]
m	meter
MWL	Mixed Waste Landfill
RETC	computer code (van Genuchten et al., 1994) used to determine the van Genuchten parameters (θ_r , θ_s , α , n , m , l , K_s) describing the hydraulic properties of soils
SNL/NM	Sandia National Laboratories/New Mexico
SWHC	Site-Wide Hydrogeologic Characterization
θ_v	volumetric moisture content [L^3/L^3]
WCR	residual volumetric moisture content [L^3/L^3]
θ_r	residual volumetric moisture content [L^3/L^3]
WCS	saturated volumetric moisture content [L^3/L^3]
θ_s	saturated volumetric moisture content [L^3/L^3]
ψ	soil moisture tension [L]
$\psi(\theta)$	soil moisture tension as a function of volumetric moisture content [L]



1.0 Introduction

Accurate modeling and successful remediation of contaminated sites require that unsaturated flow and contaminant transport be well understood and that relevant hydrologic parameters be accurately quantified. This is particularly true in the semi-arid climate at Sandia National Laboratories/New Mexico (SNL/NM), where the vadose zone can be 150 meters (m) or more in thickness (Crowson et al., 1993).

The SNL Mixed Waste Landfill (MWL) is underlain by a vadose zone extending approximately 140 m to the water table. This extensive vadose zone dictates that potential subsurface contaminant transport would initially occur as unsaturated flow. Measurement of unsaturated flow parameters and an understanding of their relationships are essential for characterizing contaminant migration.

An instantaneous profile (IP) test was conducted from December 1993 through 1995 as part of the Phase 2 RCRA Facility Investigation (RFI) of the MWL (SNL, 1993). The purpose of the IP test was to measure the hydrologic parameters controlling unsaturated flow and contaminant transport in the near-surface vadose zone at the MWL. Due to the potential for mobilizing contaminants in the MWL soils, the IP test was not conducted at the MWL itself, but 150 m to the west in uncontaminated soils analogous to those encountered at the MWL. Data from the IP test are presented in Bayliss et al., 1996, and analysis of IP test results are presented in Goering et al., 1995.

While an IP test generally yields accurate *in situ* measurements of some unsaturated hydrologic flow parameters (Marion et al., 1994), the range of values experienced during a field test is limited due to the considerable time required for residual moisture contents to be reached. Laboratory measurements of soil moisture tension and volumetric moisture content may be made over the full range of possible values and used to augment field-derived results. Field and laboratory results may also be compared to identify soil heterogeneity, structure, or incorrect assumptions inherent in the analysis of field data.

This report presents the results of laboratory tests conducted on core samples obtained from the test plot prior to the actual IP test. The computer code RETC (van Genuchten et al., 1994) was used to fit van Genuchten unsaturated flow parameters to the volumetric moisture content and soil moisture tension relationship ($\Psi(\theta)$) data measured during laboratory testing. The parameters were then used to model the hydraulic conductivity and volumetric moisture content relationship ($K(\theta)$) over the full range of possible soil moisture contents.

Laboratory testing measured water retention relationships ($\Psi(\theta)$) over extended ranges not experienced during the field test. Field data reflected *in situ* conditions difficult if not impossible to recreate in a laboratory setting. RETC predictions of $K(\theta)$ relationships based on *in situ* field data were compared with RETC predictions of $K(\theta)$ relationships based on laboratory data to determine the effects of field-scale soil structure on flow. Finally, RETC predictions based on

combined laboratory and field data sets were made to provide a more complete and accurate data set for modeling unsaturated flow and contaminant transport at the MWL.

2.0 The MWL IP Test and Sampling

This section briefly describes the IP test conducted near the MWL, sampling locations, laboratory test methods, and the computer modeling approach using RETC.

2.1 IP Test description

The MWL IP test was conducted in an uncontaminated area approximately 150 m west of the MWL in Technical Area III (Figure 1). Infiltration was constrained to one-dimensional flow using perimeter trenches filled with a 12% bentonite/soil mixture. The trenches were 0.3 m wide and 2.0 m deep. A 30 centimeter (cm) high concrete berm was built around the perimeter of the test plot to allow water to be ponded during the test. Prior to infiltration, the test plot was instrumented with Time Domain Reflectometry (TDR) probes, neutron and frequency domain probe access tubes, buried frequency domain probes, and tensiometers. Figure 2 shows the instrument locations in the IP test plot. Three neutron access tubes were installed to a depth of 3.0 m inside the test plot. Two additional neutron access tubes were installed outside the test plot to monitor potential leakage from the test plot, and to observe meteoric influences on the soil moisture profile (Goering et al., 1995).

The IP test consisted of flooding a 4.7 m by 4.7 m soil plot with 20,300 liters of water for 47.3 hours until the upper two meters of soil were saturated. Movement of the wetting front and subsequent drainage from the IP test plot were monitored with the instruments installed in the plot and a CPN Model 503DR neutron moisture meter. Volumetric moisture contents in the vertical profile continue to be monitored on a monthly basis with the neutron moisture meter.

2.2 Sample Locations

The soil core samples used in the laboratory tests were taken during installation of Borehole D in the southwest corner of the IP test plot, adjacent to instrument cluster A (Figure 2). Core samples were collected from 0 to 269 cm below ground surface (bgs). A two-inch split-spoon sampler was manually driven into the ground to collect the core samples. Due to the dry, friable nature of the soils, completely undisturbed and intact soil core samples were not always obtained.

2.3 Sample Preparation and testing

Individual samples were taken from 3 to 15 cm depth intervals. Where necessary, samples were packed to estimated *in situ* bulk density in two-inch brass or stainless steel rings. Seventeen samples were tested in the SNL Environmental Restoration Project Hydrology Testing Laboratory for saturated hydraulic conductivity (K_s) and the relationships between soil moisture tensions and volumetric moisture content ($\Psi(\theta)$).

$\Psi(\theta)$ relationships for the core samples were measured using a pressure pot/ceramic plate apparatus as specified in *Methods Of Soil Analysis* (MOSA), No. 9, Part 1, pp. 637-638 (Klute (ed) 1986). Soil moisture tensions in the pressure pot were varied from 6 to 15,300 cm H₂O. The saturated hydraulic conductivity of the core samples was measured using the constant-head method described in MOSA, No. 9, Part 1, pp. 694-700.

3.0 Results

The IP field infiltration test and the laboratory tests of soil core samples were conducted to study the hydraulic properties of the near-surface vadose zone beneath the MWL. The parametric fitting program RETC (van Genuchten et al., 1994) was used to quantify hydraulic properties.

3.1 Fitting of van Genuchten Parameters and Modeling of $K(\theta)$ Relationships

$\Psi(\theta)$ data from laboratory tests of IP samples and $K(\theta)$ data derived from the Hillel one-step analysis of the IP test data (Hillel, et al., 1972 and Goering et al., 1995) were used as inputs to the parameter-fitting program RETC (van Genuchten et al., 1994). RETC fits seven parameters (θ_s , θ_r , α , n , m , l , and K_s) to supplied data. After fitting, the program uses the parameters to predict the full range of $\Psi(\theta)$ and $K(\theta)$ relationships.

Parameters were fitted using an iterative approach. Initial parameter estimates were input from expected parameter values for the soil samples (Carsel and Parrish, 1988, and Rawls, et al., 1982). The RETC program was then allowed to fit all parameters to known values (laboratory or field data sets). R-squared and the sum of squares of observed-minus-fitted values were checked to determine fit accuracy. The correlation matrix was also inspected to detect non-unique relationships between parameters. Non-unique relationships not prevented by restrictions on solution methods (e.g., forcing $m = 1 - 1/n$) were then eliminated by arbitrarily fixing one of the parameters involved at a reasonable or tested value (van Genuchten et al., 1994). Once parameters were well-fitted and non-unique relationships eliminated, the entire process was repeated with different original input parameters to insure that the values obtained were global solutions and did not represent local minimums. The parametric model of van Genuchten was then used by RETC to predict the full $\Psi(\theta)$ relationship. The theoretical pore-size distribution model of Mualem was used to predict the full $K(\theta)$ relationship for the sample (van Genuchten et al., 1994).

Neither $\Psi(\theta)$ nor $K(\theta)$ data alone will fit all seven van Genuchten parameters; e.g., $\Psi(\theta)$ data from laboratory testing will not fit K_s , and $K(\theta)$ data from the IP test will not fit α . If simultaneous $K(\theta)$ and $\Psi(\theta)$ data are not available, some parameter values will have to be measured, assumed, or taken from the literature. However, combining laboratory $\Psi(\theta)$ and field $K(\theta)$ data provides a complete fitting of all seven parameters (van Genuchten et al., 1994). Parameters fitted using only laboratory $\Psi(\theta)$ data are presented in Table 1. Parameters fitted using only *in situ* $K(\theta)$ data are given in Table 2. Fitted parameters using both data sets are presented in Table 3.

Graphs showing RETC predictions of $K(\theta)$ and $\psi(\theta)$ hydraulic functions that are based only on laboratory-tested samples are presented in Section 1, Appendix A. Graphs showing RETC predictions of extended $K(\theta)$ relationships from IP *in situ* $K(\theta)$ data are presented in Section 2, Appendix A. Graphs showing RETC-predicted $K(\theta)$ relationships from combined laboratory and field data are presented in Section 3, Appendix A. For comparative purposes, the $K(\theta)$ relationships predicted from field and laboratory data alone are also shown on the graphs of $K(\theta)$ relationships from combined data.

3.2 Saturated Hydraulic Conductivity (K_s) Predicted by RETC Modeling

Figure 3 presents graphs of K_s with depth from laboratory testing, *in situ* IP field data, and combined laboratory and IP data. Literature values of K_s for soils similar to those at the IP test site (loam, sandy loam, silts, and clayey silts) range from 10^{-7} centimeters per second (cm/s) to 10^3 cm/s (Freeze and Cherry, 1979). Because both laboratory testing and IP flow was essentially perpendicular to the layered heterogeneity of the alluvial deposits studied, effective saturated hydraulic conductivity (K_{eff}) was calculated as:

$$K_{eff} = \frac{\sum z_i}{\sum (z_i / K_i)}, \text{ where } \begin{array}{l} K_{eff} = \text{effective hydraulic conductivity} \\ z_i = \text{depth of the interval} \\ K_i = \text{hydraulic conductivity of the interval} \end{array}$$

Laboratory measurements of K_s from core samples obtained from the IP test site ranged from 2.0×10^{-7} cm/s to 3.0×10^{-4} cm/s (Table 1). The calculated K_{eff} from laboratory-measured samples was 2.9×10^{-6} cm/s. K_s predicted by RETC based on *in situ* $K(\theta)$ data ranged from 2.0×10^{-5} cm/s to 2.3×10^{-3} cm/s (Table 2). The calculated K_{eff} from IP field data was 8.6×10^{-5} cm/s. RETC-predicted values of K_s based on the data set combining laboratory and field measurements ranged from 2.4×10^{-3} cm/s to 9.9×10^{-3} cm/s (Table 3). The calculated K_{eff} based on combined laboratory and IP field measurements was 4.6×10^{-3} cm/s.

Laboratory measurement of K_s may reflect significant sources of error such as loss of *in situ* structure and heterogeneity, incorrect boundary conditions, or inaccurate bulk density (if re-packed from disturbed media). In this study, laboratory measurements of K_s were generally lower than K_s predictions from data gathered during the IP test (Figure 3). Because of the noncohesive nature of soils at the IP test site, samples could not always be collected in a perfectly intact, undisturbed condition. In addition, the small, two-inch diameter of the core samples reduced the ability of the samples to reflect *in situ* flow features such as macropores and heterogeneity.

The effect of soil structure on K_s can be illustrated by comparing the RETC-predicted K_s values from laboratory tests with field-derived values from the IP test (Figure 4). The greatest divergence between laboratory and field predictions of K_s occurs near the saturated end of the curve, where structure and macropore flow is most possible. As the soil moisture content

decreases, macropore and fracture flow is less likely, and the difference between laboratory and field results is much less apparent.

Predicted K_s values from IP test data are lower than K_s values from combined laboratory and IP data due to the constraints of the IP test. In a short-term ponded infiltration event such as the IP test, the vertical profile rarely reaches complete saturation because of entrapped air in the soil pores. The entrapped air decreases both the measured saturation (Figure 5) and the hydraulic conductivity (Figure 3). In the laboratory environment, deaerated water, vacuum saturation techniques, and the lack of time constraints can eliminate or greatly reduce the quantity of entrapped pore air. As a result, RETC-predictions from IP field data of the $K(\theta)$ relationship at the saturated or near-saturated range yield lower hydraulic conductivity. When laboratory and field data are combined, the higher saturated moisture contents of laboratory testing are reflected in higher predictions of K_s (see Figures 3 and 5).

3.3 Unsaturated Hydraulic Conductivity

Differences between laboratory, field, and combined laboratory and field predictions of hydraulic conductivity are less significant with decreasing volumetric moisture content (Figure 4). This is probably due to the reduction in preferential flow as fractures and macropores become unsaturated at lower soil moistures.

Based on more than 160 samples collected from boreholes extending to over 137 m bgs at sites at SNL/NM (SNL, 1996), a conservative estimate of the average native volumetric moisture content in the vadose zone below the MWL is approximately ten percent. At this moisture content, average unsaturated hydraulic conductivity ($K(\theta)$) values for the combined laboratory and IP field data sets are on the order of 10^{-11} cm/s, with maximum values on the order of 10^{-10} cm/s (Figure 6).

4.0 Conclusions

Data sets combining laboratory and field data are superior to laboratory or field data sets alone. Modeling based on data from laboratory tests may under predict $K(\theta)$ due to loss of structure, heterogeneity, or inaccurate boundary conditions. Field infiltration tests may accurately simulate small, short-term events such as spills, but may not reflect the full saturation and greater hydraulic conductivity associated with long-term leakage; for example, a failed settling-pond liner or leaking water line. When modeling soil moisture characteristics and unsaturated hydraulic conductivity data using the computer program RETC, the most accurate predictions of hydraulic conductivity are based on data sets that combine field and laboratory data.

Combining laboratory and field data expresses the full range and most accurate predictions of $\psi(\theta)$ and $K(\theta)$ relationships. RETC predictions of K_{eff} through the near-surface vadose zone was

predicted to be 4.6×10^{-3} cm/s using combined laboratory and IP field data, approximately one and one-half orders of magnitude greater than predictions based on field data alone (8.6×10^{-5} cm/s), and more than three orders of magnitude greater than values measured in laboratory tests (2.9×10^{-6} cm/s).

Comparing RETC predictions based on laboratory data with predictions based on field data illustrates the apparent influence of *in situ* field-scale structure and preferential flow. The higher predicted values of K_s based on field data alone compared to simulations derived from laboratory data alone suggest that soil structure not investigated during testing of laboratory samples may contribute to preferential flow when soil moisture contents approach saturation (Figure 4).

At the approximate native moisture contents existing in the vadose zone below the MWL ($\theta_v \cong 0.10$), RETC predictions of maximum and average $K(\theta)$ based on either field data, laboratory data, or combined laboratory and field data are all on the order of 10^{-10} cm/s (see Figures 4 and 6). Assuming a unit gradient with depth and a maximum unsaturated hydraulic conductivity of 10^{-10} cm/s, the maximum steady-state areal recharge rate in the vicinity of the MWL is calculated to be 10^{-10} cm/s (1.2×10^{-3} inches per year). This is approximately 0.02% of the annual precipitation rate at SNL/NM, and implies that the potential for aqueous recharge through the vadose zone to groundwater is very low, exclusive of preferential flow.

5.0 References

- Bayliss, S., Goering, T. J., McVey, M. D., Strong, W. R., and J. L. Peace. 1996. Preliminary Data from an Instantaneous Profile Test Conducted Near the Mixed Waste Landfill, Technical Area 3, Sandia National Laboratories/New Mexico. SAND96-0813
- Carsel, R. F. and R. S. Parrish. 1988. Developing joint probability distributions of soil water retention characteristics. *Water Resour. Res.* vol. 24.
- Crowson, D., Gibson, J. D., Haase, C. S., Holt, R., Hyndman, D., Krumhansl, J., Lauffer, F., McCord, J. P., McCord, J. T., Neel, D., Parsons, A. M., and R. Thomas. 1993. SNL Site-Wide Hydrogeologic Characterization Project Calendar Year 1992 Annual Report. SNL, Albuquerque, NM.
- Freeze, R. A., and Cherry, J. A., (1979), *Groundwater*, Prentice-Hall, Inc, Englewood Cliffs, New Jersey.
- Goering, T. J., McVey, M. D., Strong, W. R., Nguyen, H. A., and J. L. Peace. 1995. Analysis of Instantaneous Profile Test Data from Soils Near the Mixed Waste Landfill, Technical Area 3, Sandia National Laboratories/New Mexico. Sand Report Sand95-1637. Sandia National Laboratories, Albuquerque, New Mexico.
- Hillel, D., Krentos, V. D., and Y. Stylianou. 1972. Procedure and test of an internal drainage method for measuring soil hydraulic characteristics *in situ*. *Soil Science.* vol. 114, No. 5.
- Klute, A. (ed). *Methods of Soil Analysis, Part 1, Physical and Mineralogical Methods.* 1986. 2nd Edition, Soil Science Society of America, Inc. Madison, WI.
- Marion, J. M., Or, D., Rolston, D. E., Kavvas, M. L., and J. W. Biggar. 1994. Evaluation of Methods for Determining Soil-Water Retentivity and Unsaturated Hydraulic Conductivity. *Soil Science.* Vol. 158, No. 1.
- Rawls, W. J., Brackensiek, D. L., and K. E. Saxton. 1982. Estimating soil water properties. *Transactions, ASAE.* vol. 25(5).
- SNL. 1993. Mixed Waste Landfill Phase 2 RCRA Facility Investigation Work Plan. Prepared by Sandia National Laboratory Environmental Restoration Program for the United States Department of Energy, Albuquerque Operations Office.
- SNL. 1996. SWHC 1995 Calendar Year Annual Report. Environmental Restoration Project, DOE, Albuquerque Operations Office.
- Van Genuchten, M. Th., Leij, F. J., and S. R. Yates. 1994. RETC: Quantifying the hydraulic functions of unsaturated soils. Computer program IGWMC-FOS 55. International Groundwater Modeling Center, Golden, CO.

Tables

Table 1. RETC-derived parameters from $\psi(\theta)$ data of laboratory-tested samples. K_s and l were fixed at laboratory-measured values in these simulations.

Sample	Average Depth (cm)	WCR (cm ³ /cm ³)	WCS (cm ³ /cm ³)	α (1/cm)	n (-)	m (-)	l (-)	K_s , RET (cm/s)	R ²
IP-300	0.8	0.05	0.38	0.008	1.35	=1-1/n	0.50	3.0E-04	0.957
IP-301	23.0	0.04	0.40	0.150	1.36	=1-1/n	0.50	1.0E-04	0.994
IP-302	35.5	0.07	0.43	0.017	1.33	=1-1/n	0.50	1.0E-04	0.980
IP-303	45.5	0.14	0.39	0.014	1.42	=1-1/n	0.50	3.0E-04	0.983
IP-304	66.6	0.09	0.38	0.015	1.55	=1-1/n	0.50	3.0E-04	0.990
IP-305	76.5	0.06	0.35	0.019	1.39	=1-1/n	0.50	1.0E-04	0.996
IP-306	86.5	0.06	0.32	0.012	1.01	0.18	0.50	2.0E-05	0.981
IP-307	96.5	0.17	0.35	*	1.21	=1-1/n	0.50	7.0E-07	0.923
IP-308	106.5	0.08	0.41	0.013	1.41	=1-1/n	0.50	7.0E-05	0.996
IP-309	137.5	0.08	0.31	0.005	1.22	=1-1/n	0.50	2.0E-06	0.982
IP-310	147.5	0.04	0.33	0.014	1.19	=1-1/n	0.50	3.0E-06	0.986
IP-311	158.5	0.10	0.35	0.160	1.14	=1-1/n	0.50	2.0E-07	0.920
IP-312	167.5	0.11	0.45	0.014	1.07	=1-1/n	0.50	4.0E-05	0.997
IP-313	179.0	0.11	0.42	*	1.48	=1-1/n	0.50	3.0E-04	0.956
IP-314	188.0	0.05	0.35	0.005	1.26	=1-1/n	0.50	3.0E-04	0.986
IP-315	203.5	0.06	0.45	0.019	1.33	=1-1/n	0.50	3.0E-05	0.998
IP-318	228.5	0.03	0.45	0.019	1.01	=1-1/n	0.50	2.0E-05	0.996
IP-320	261.5	0.08	0.37	0.012	1.69	0.33	0.50	1.0E-04	0.997

	<u>WCR</u>	<u>WCS</u>	<u>α</u>	<u>n</u>	<u>m</u>	<u>K_s</u>
Minimum	0.030	0.310	0.005	1.010	0.180	2.0E-07
Maximum:	0.170	0.450	0.160	1.690	0.327	3.0E-04
Average:	0.079	0.383	0.031	1.301	0.254	1.2E-04
Standard Deviation:	0.037	0.045	0.049	0.182	0.104	1.2E-04

* RETC could not fit a reasonable value

Table 2. RETC-derived parameters from *in situ* $K(\theta)$ data derived during the IP test. Because $K(\theta)$ data does not reflect air entry pressures, the van Genuchten parameter related to air entry pressure, α , was necessarily fixed.

Sample	Average Depth (cm)	WCR (cm ³ /cm ³)	WCS (cm ³ /cm ³)	α (1/cm)	n (-)	m (-)	l (-)	K_s (cm/s)	R^2
015-045s	30	0.05	0.24	0.013	1.39	=1-1/n	0.50	2.3E-05	0.951
045-075s	60	0.07	0.28	0.010	1.42	=1-1/n	0.50	2.0E-04	0.994
075-105s	90	0.08	0.31	0.010	1.74	=1-1/n	0.50	1.0E-04	0.988
105-135s	120	0.08	0.32	0.010	1.19	=1-1/n	8.38	2.0E-03	0.992
135-165s	150	0.10	0.29	0.010	1.41	=1-1/n	0.50	1.0E-04	0.985
165-195s	180	0.10	0.42	0.010	1.40	=1-1/n	0.50	9.0E-04	0.987

	<u>WCR</u>	<u>WCS</u>	<u>α</u>	<u>n</u>	<u>m</u>	<u>K_s</u>
Minimum	0.037	0.045	0.010	0.182	0.104	2.3E-05
Maximum:	0.170	0.450	0.160	1.735	0.327	2.0E-03
Average:	0.085	0.304	0.034	1.303	0.228	4.3E-04
Standard Dev	0.038	0.119	0.049	0.454	0.114	6.5E-04

Table 3. RETC-derived parameters from combined laboratory $\psi(\theta)$ and *in situ* $K(q)$ data.

Sample	Average Depth (cm)	WCR (cm ³ /cm ³)	WCS (cm ³ /cm ³)	α (1/cm)	n (-)	m (-)	l (-)	K_s (cm/s)	R^2
015-045s	30	0.08	0.40	0.011	1.4299	1-1/n	0.0001	6.1E-03	0.996
045-075s	60	0.08	0.38	0.015	1.47	1-1/n	0.50	3.2E-03	0.997
075-105s	90	0.11	0.36	0.008	1.4216	1-1/n	8.1144	2.4E-03	0.996
105-135s	120	0.07	0.36	0.029	1.2029	1-1/n	4.039	5.5E-03	0.993
135-165s	150	0.08	0.36	0.046	1.381	1-1/n	0.0008	7.5E-03	0.992
165-195s	180	0.10	0.40	0.066	1.2843	1-1/n	-3.7545	9.9E-03	0.985

	<u>WCR</u>	<u>WCS</u>	<u>α</u>	<u>n</u>	<u>m</u>	<u>K_s</u>
Minimum	0.037	0.045	0.008	0.182	0.104	2.3E-05
Maximum:	0.170	0.450	0.160	1.735	0.327	9.9E-03
Average:	0.084	0.316	0.043	1.186	0.193	3.8E-03
Standard Dev	0.038	0.130	0.045	0.483	0.106	3.3E-03

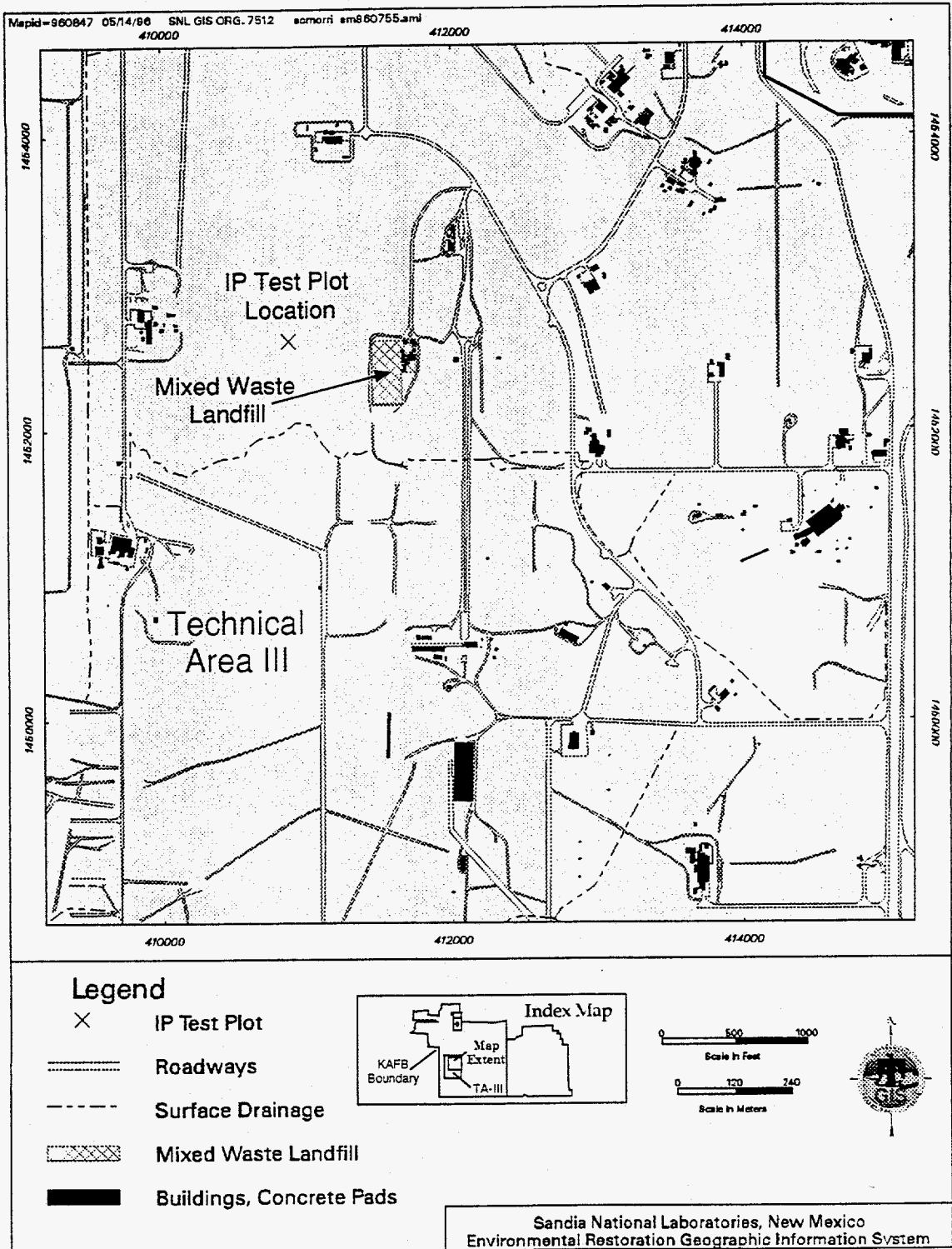


Figure 1. Instantaneous profile test plot location.

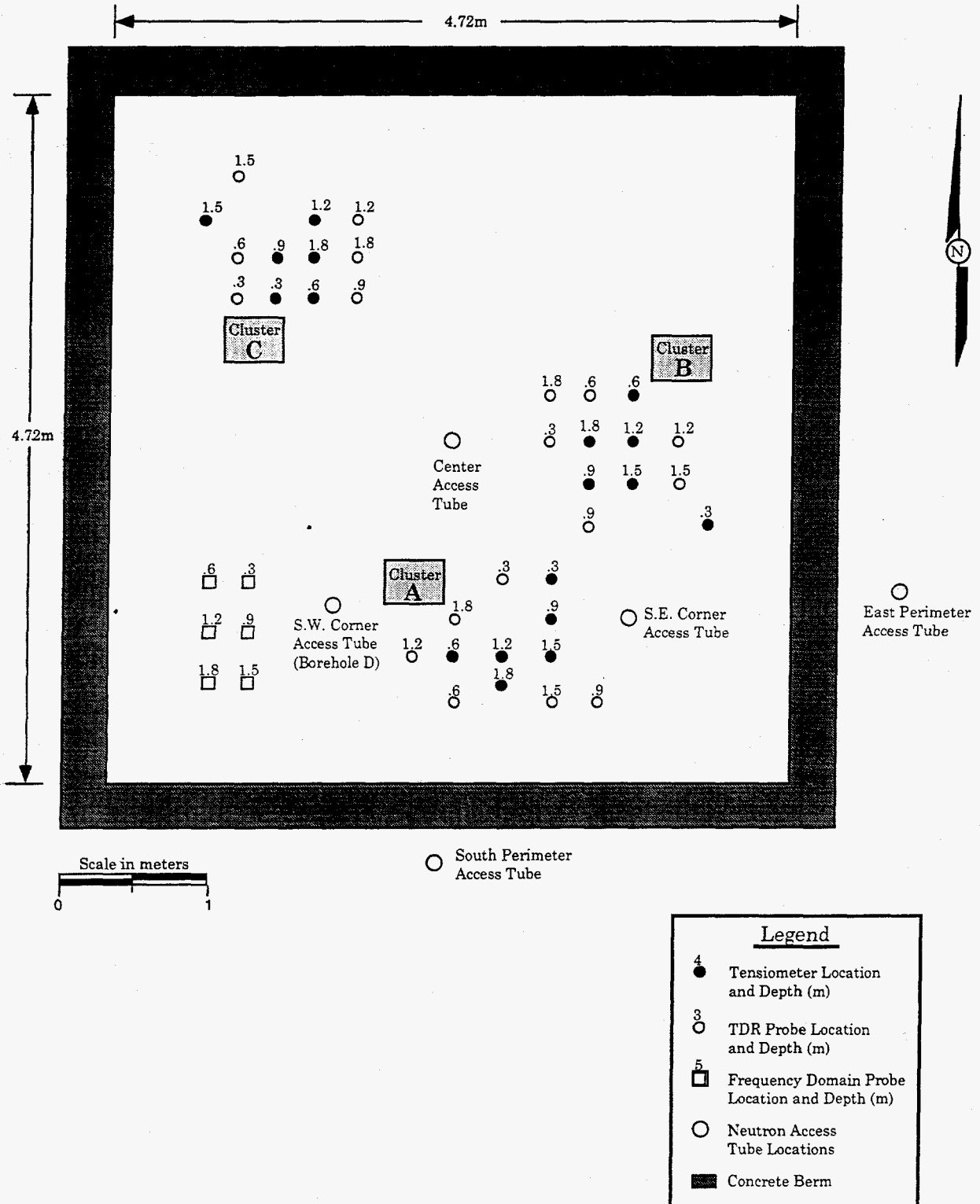


Figure 2. Instrument Locations in the IP test plot. Numbers above symbols indicate installation depth below ground surface.

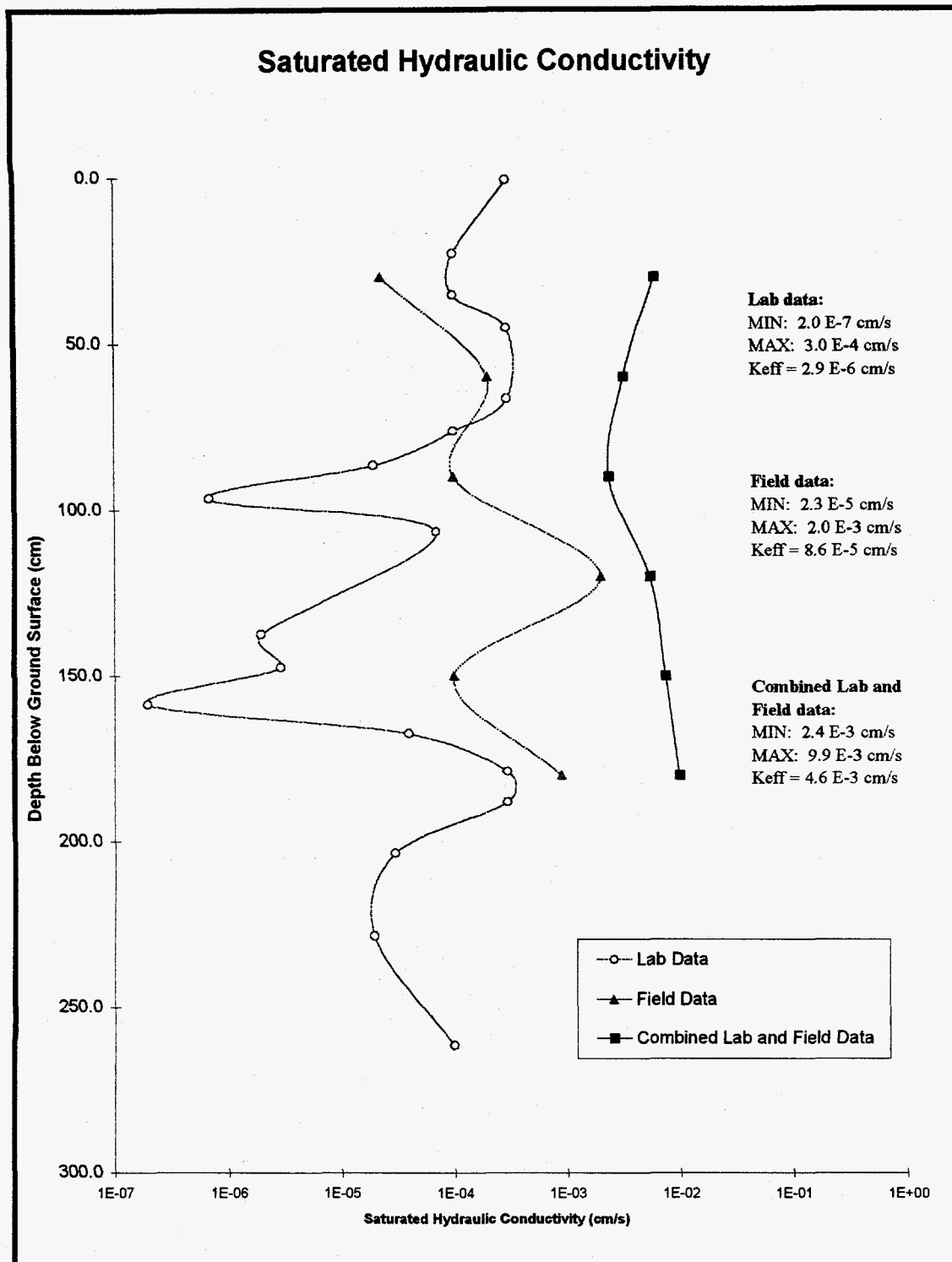


Figure 3. Saturated hydraulic conductivity with depth. Note that the average predicted value from the combined laboratory and IP field data exceeds that from field data alone by more than an order of magnitude and exceeds laboratory values by three orders of magnitude.

**Laboratory-Tested and RETC-Modeled Field Hydraulic Conductivity,
45 - 75 Centimeters Below Ground Surface**

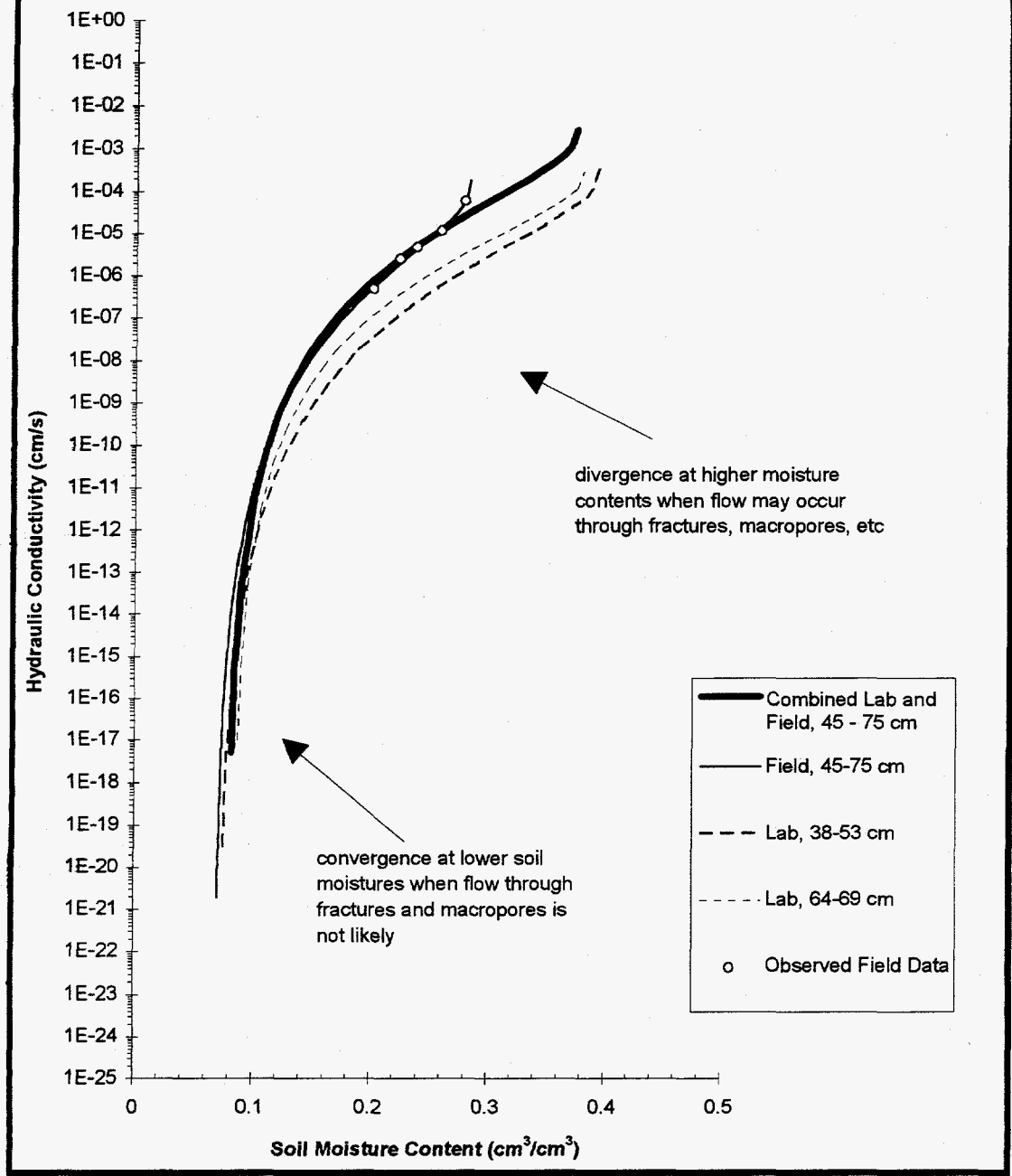


Figure 4. RETC-predicted hydraulic conductivity-moisture content relationships based on field, laboratory, and combined field and laboratory data. Lower hydraulic conductivity values from laboratory testing are observed at higher moisture contents. The divergence at higher moisture contents and the convergence at lower moisture contents suggests that preferential flow through soil structure (macropores and fractures) may occur if moisture contents approach saturation.

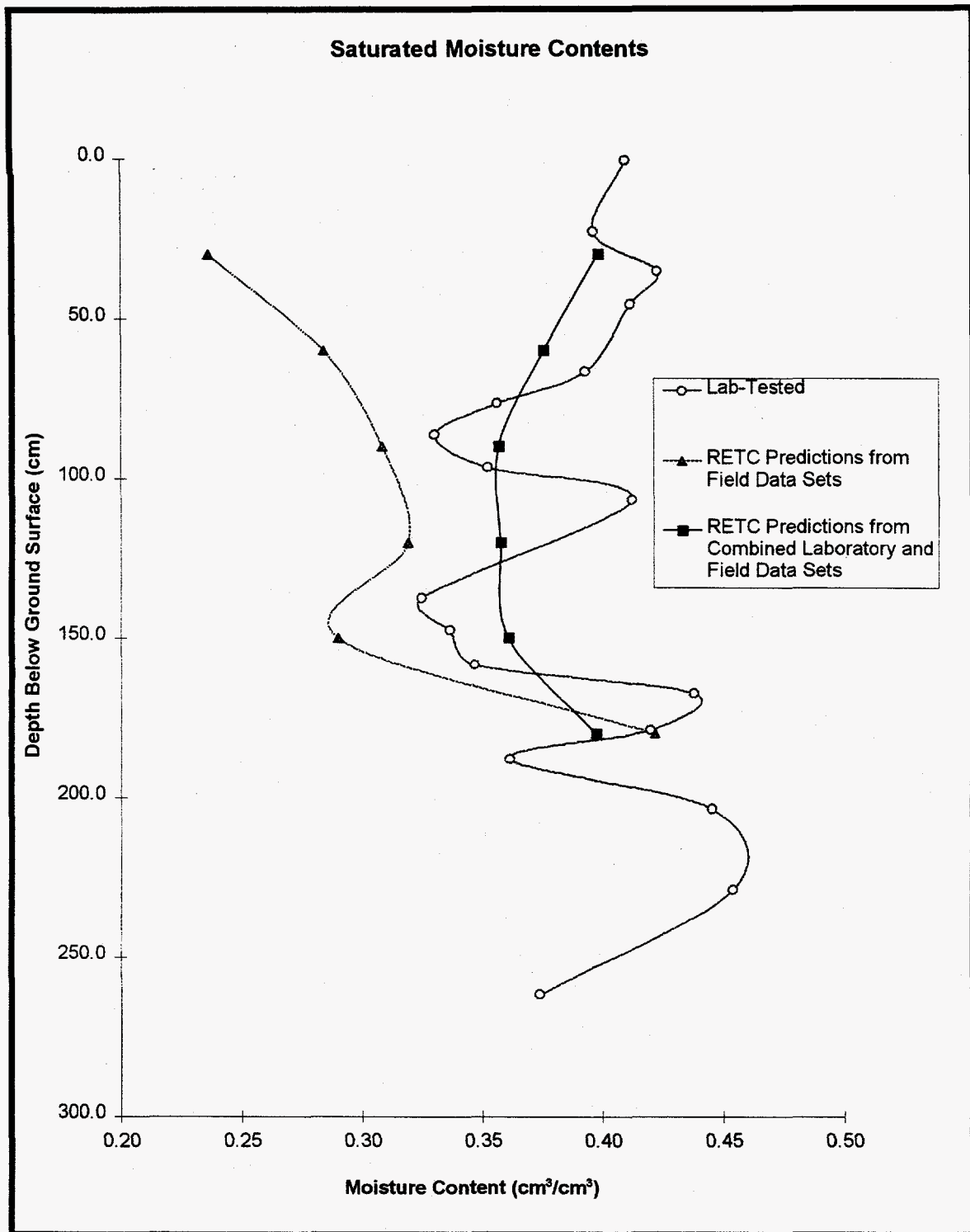


Figure 5. Laboratory-tested and RETC prediction of saturated moisture content based on IP field and combined field and laboratory data sets. Note that for all but the deepest interval, saturated moisture contents are least for field data. This yielded lower RETC predictions of saturated hydraulic conductivity from field data (see Figure 3).

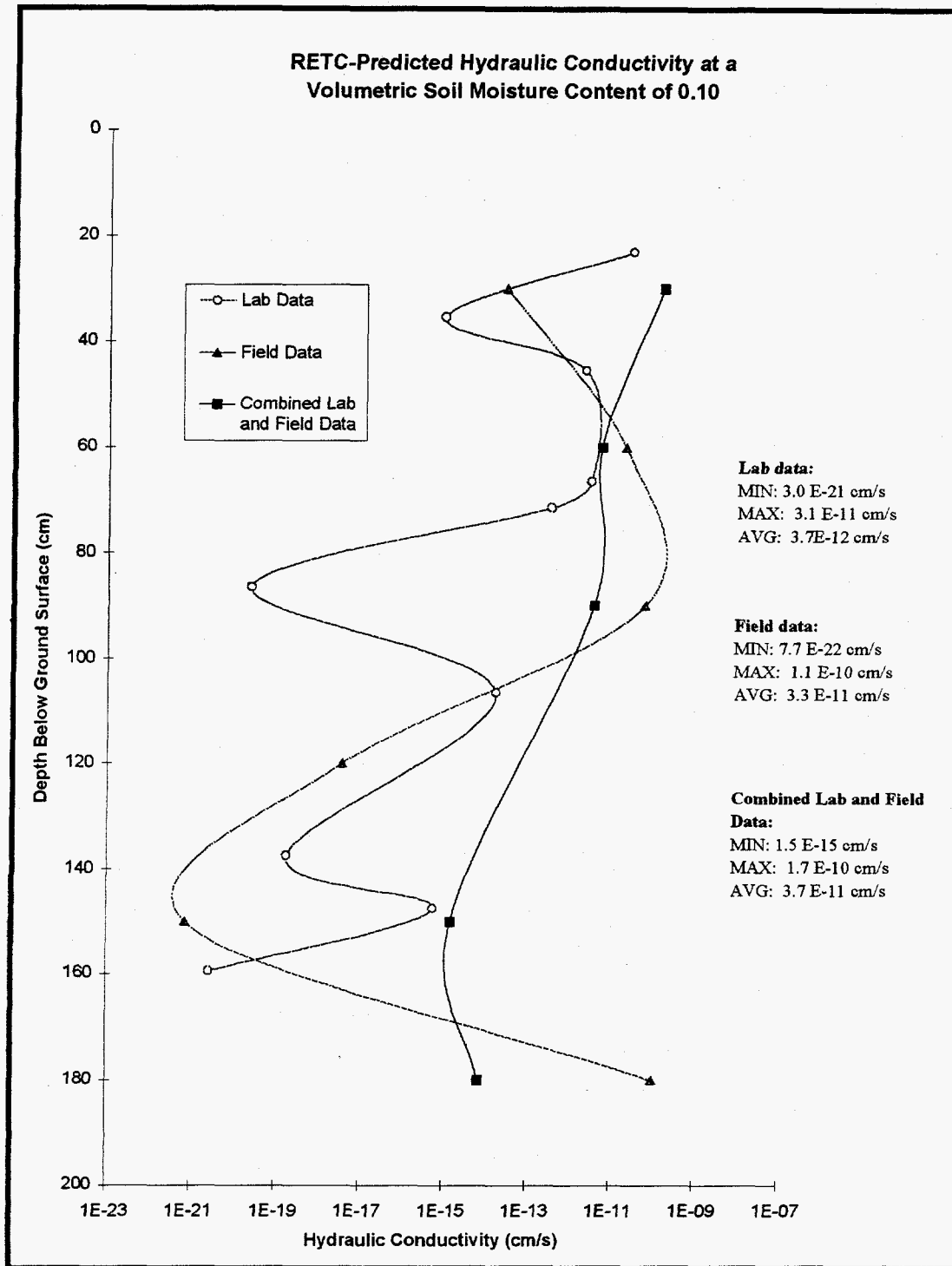
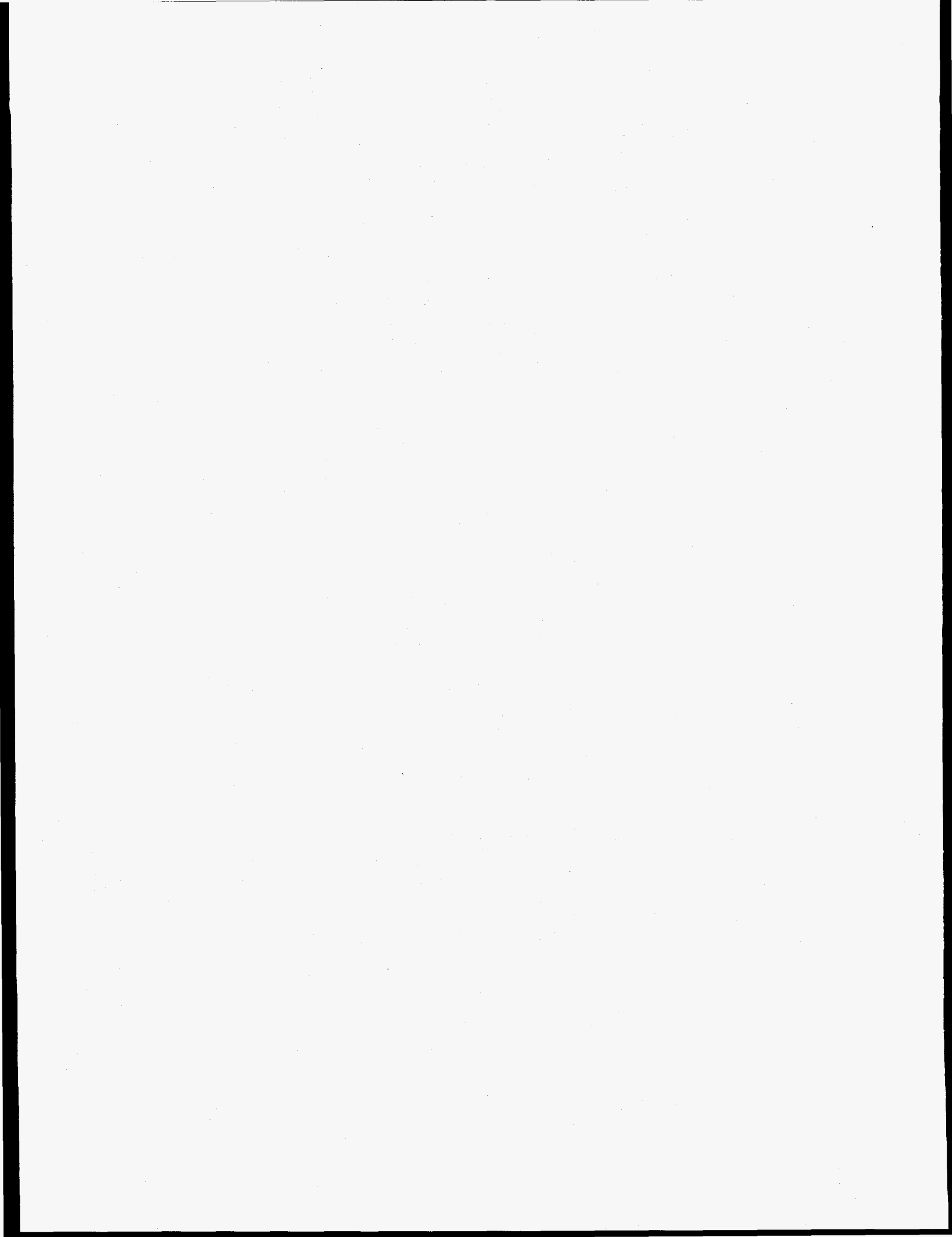


Figure 6. Hydraulic conductivity profile at a volumetric moisture content of 10 percent. At a volumetric moisture content of ten percent, the differences between RETc predictions from the three data sets are less definite than at saturated moisture contents (Figure 3). Regardless of the data set used, the predicted hydraulic conductivity is of so low a magnitude that aqueous transport from the MWL to groundwater is unlikely.



APPENDIX A

RETC Predictions of $\psi(\theta)$ and $K(\theta)$ Relationships for Soils in the Vadose Zone Near the Mixed Waste Landfill

Contents

Section 1.0	Graphs of $\psi(\theta)$ and $K(\theta)$ relationships based on laboratory testing of samples	A-2
Section 2.0	Graphs of $K(\theta)$ relationships based on data collected <i>in situ</i> during the Instantaneous Profile (IP) test	A-21
Section 3.0	Graphs of $K(\theta)$ relationships based on combined laboratory and field data	A-25

All graphs represent predictions made using the RETC computer code (van Genuchten et al., 1994). Field data were obtained during the Sandia National Laboratories/New Mexico Mixed Waste Landfill Instantaneous Profile Test (Goering et al., 1995).

References

- Goering, T. J., McVey, M. D., Strong, W. R., Nguyen, H. A., and J. L. Peace. 1995. Analysis of Instantaneous Profile Test Data from Soils Near the Mixed Waste Landfill, Technical Area 3, Sandia National Laboratories/New Mexico. Sand Report Sand95-1637. Sandia National Laboratories, Albuquerque, New Mexico.
- Van Genuchten, M. Th., Leij, F. J., and S. R. Yates. 1994. RETC: Quantifying the hydraulic functions of unsaturated soils. Computer program IGWMC-FOS 55. International Groundwater Modeling Center, Golden, CO.

Section 1.0 Graphs of RETC $\psi(\theta)$ and $K(\theta)$ relationships from data derived from laboratory testing of samples

RETC simulations of soil moisture retention relationships are presented in this section. The RETC fits of lab $\psi(\theta)$ data for a sample are presented, along with graphs of the RETC predictions of the $K(\theta)$ relationship for that same sample, on pages A-3 through A-20. The results for the eighteen samples tested are shown. Samples are presented in order of increasing depth.

Sample number (e.g., IP 300), depth, R-squared value for the fit, and van Genuchten parameters are noted for each sample. If during the fitting process, it was necessary to fix a parameter value, its fixed value is noted; e.g., "WCR: 0.05." If the RETC program was allowed to fit the parameter value, both the initial estimate used and the final fitted value are shown. For example, "WCR: 0.05 => 0.11" indicates that the program fitted a final volumetric residual moisture content value of 0.11 from an initial estimate of 0.05.

Nomenclature

Rsq	the R-squared value for the fit.
WCR	residual volumetric moisture content. [L^3/L^3]
WCS	saturated soil moisture content. [L^3/L^3]
α	the van Genuchten parameter related to the air entry pressure. [$1/L$]
n	the "n" van Genuchten fitting parameter. [-]
m	the "m" van Genuchten fitting parameter. [-]
l	the "l" van Genuchten parameter. [-]
K_s	saturated hydraulic conductivity. [L/T]
$K(\theta)$	unsaturated hydraulic conductivity as a function of soil moisture content. [L/T]
$\psi(\theta)$:	the model used by the RETC program to predict the soil matric tension/soil moisture content relationship. "van" denotes the van Genuchten solution, "B.C." indicates the Brooks/Corey model was used.
$K(\psi)$:	the model used to predict the unsaturated hydraulic conductivity. "Mualem" indicates the Mualem model was used. "Burdine" indicates that the Burdine model was used.
bgs	below ground surface.

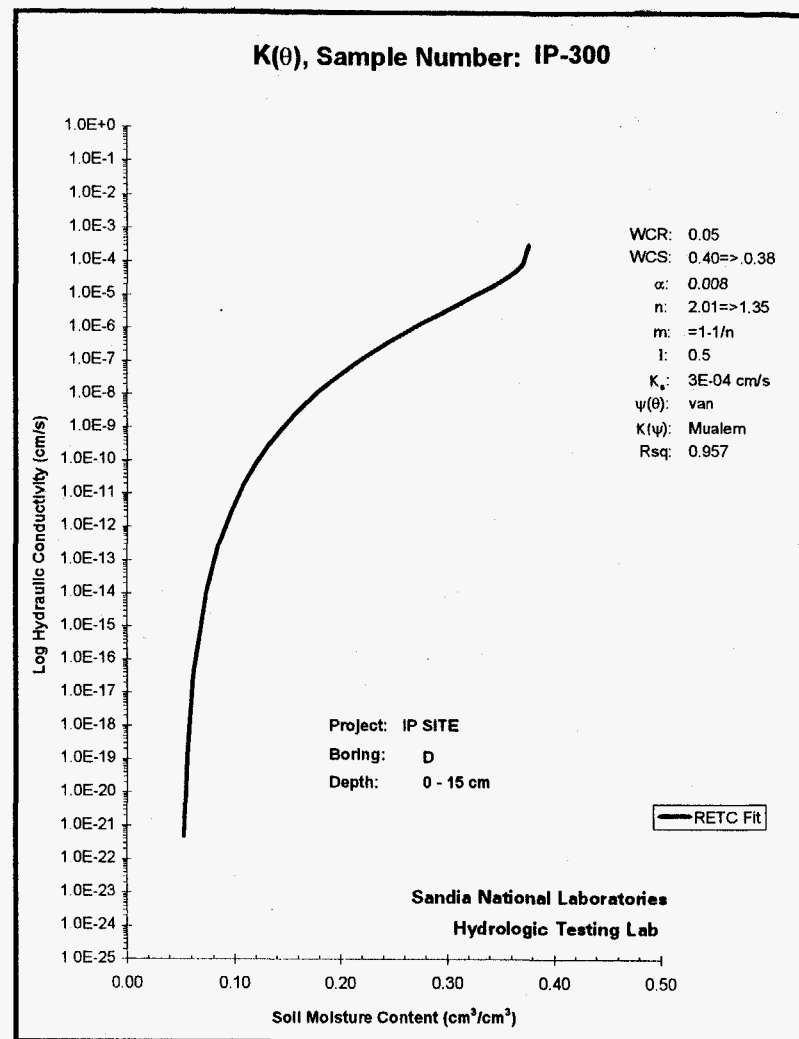
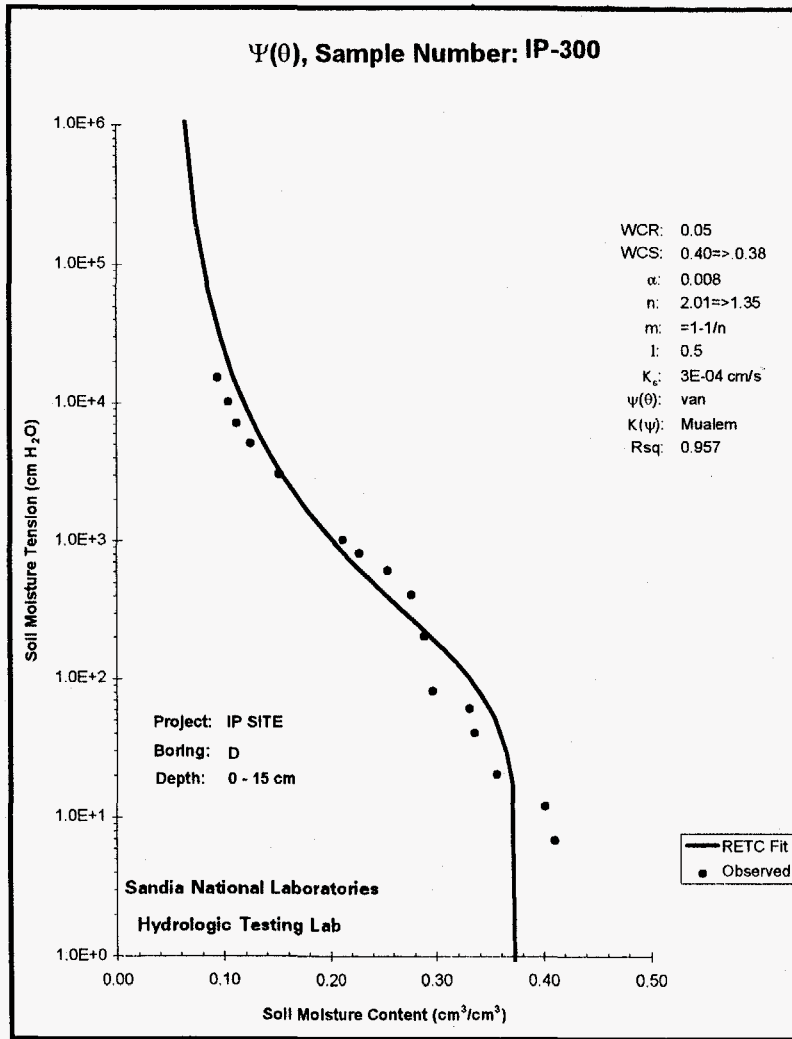


Figure A-1. RETC simulations of $\psi(\theta)$ and $K(\theta)$ relationships for the laboratory-tested sample from 0 - 15 cm bgs.

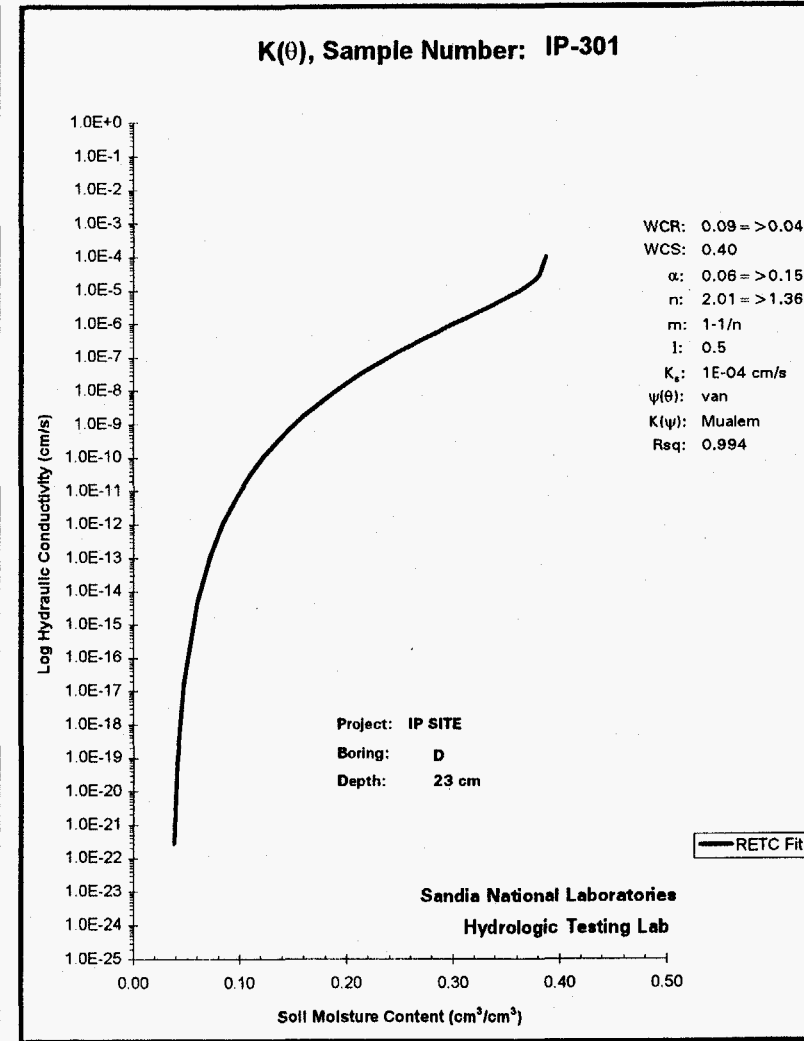
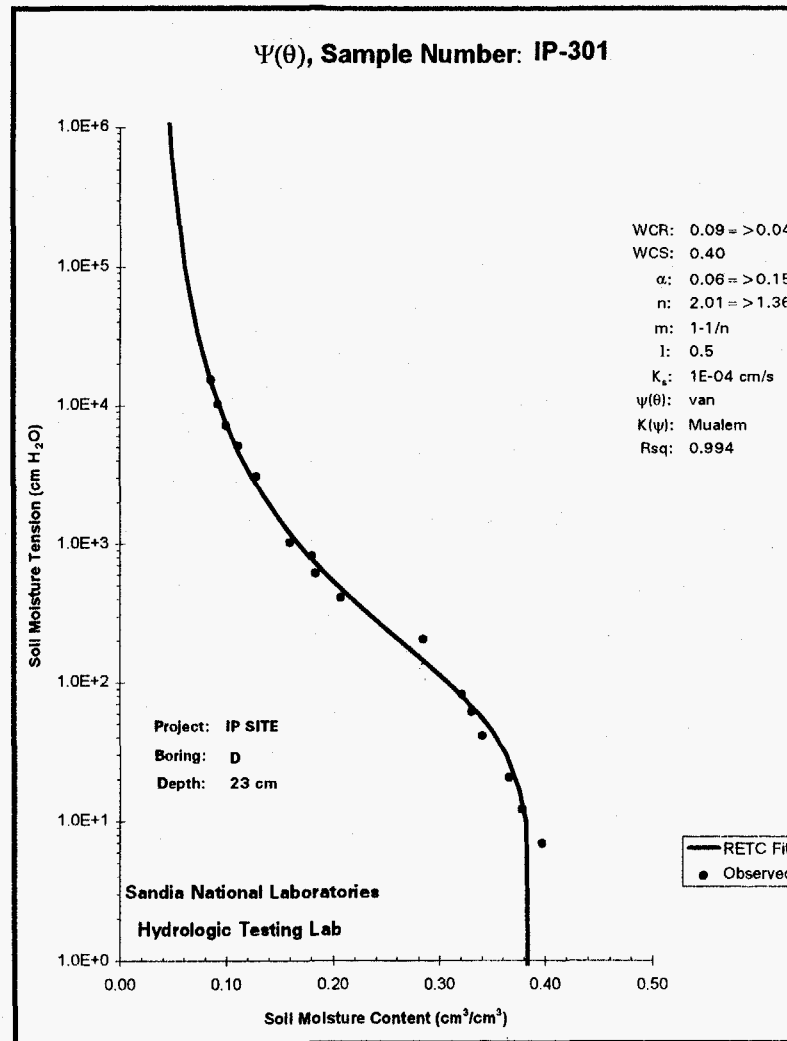


Figure A-2. RETC simulations of $\psi(\theta)$ and $K(\theta)$ relationships for the laboratory-tested sample from 33 cm bgs.

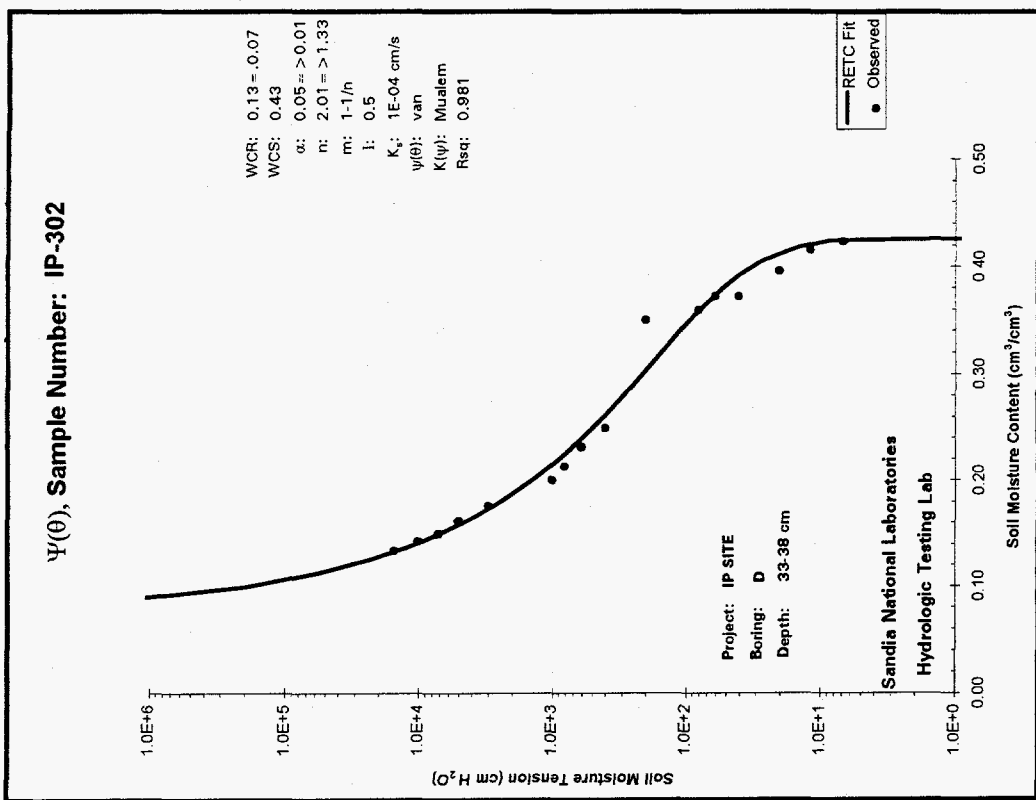
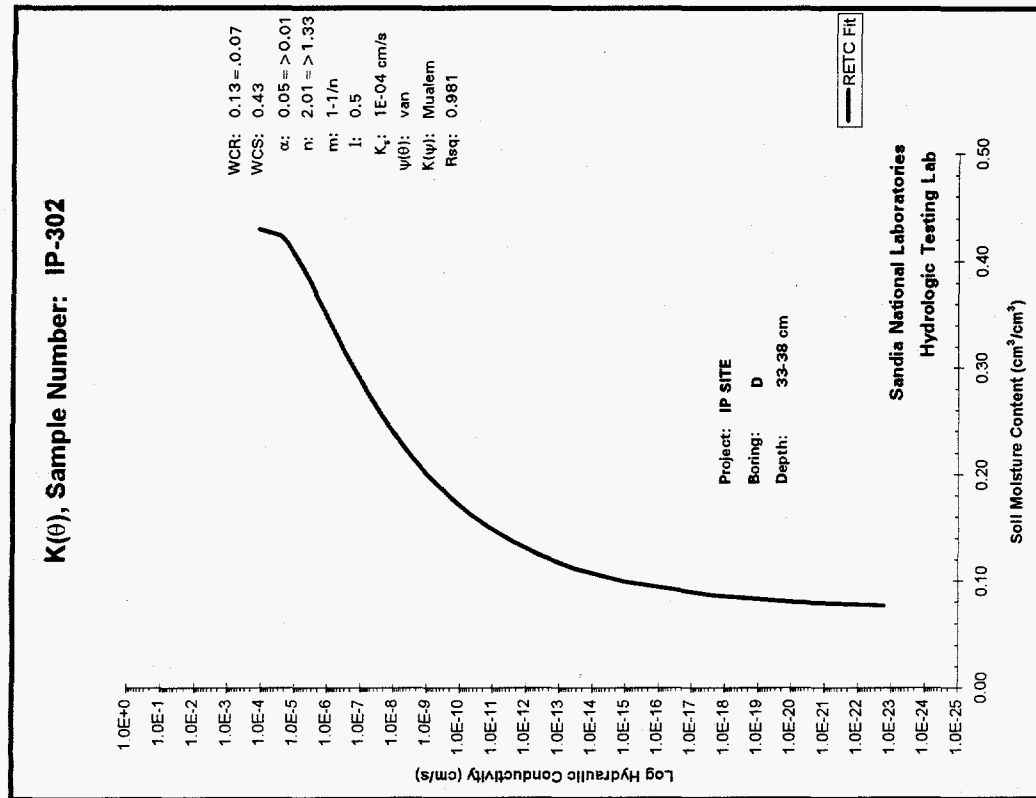


Figure A-3. RETC simulations of $\psi(\theta)$ and $K(\theta)$ relationships for the laboratory-tested sample from 33 - 38 cm bgs.

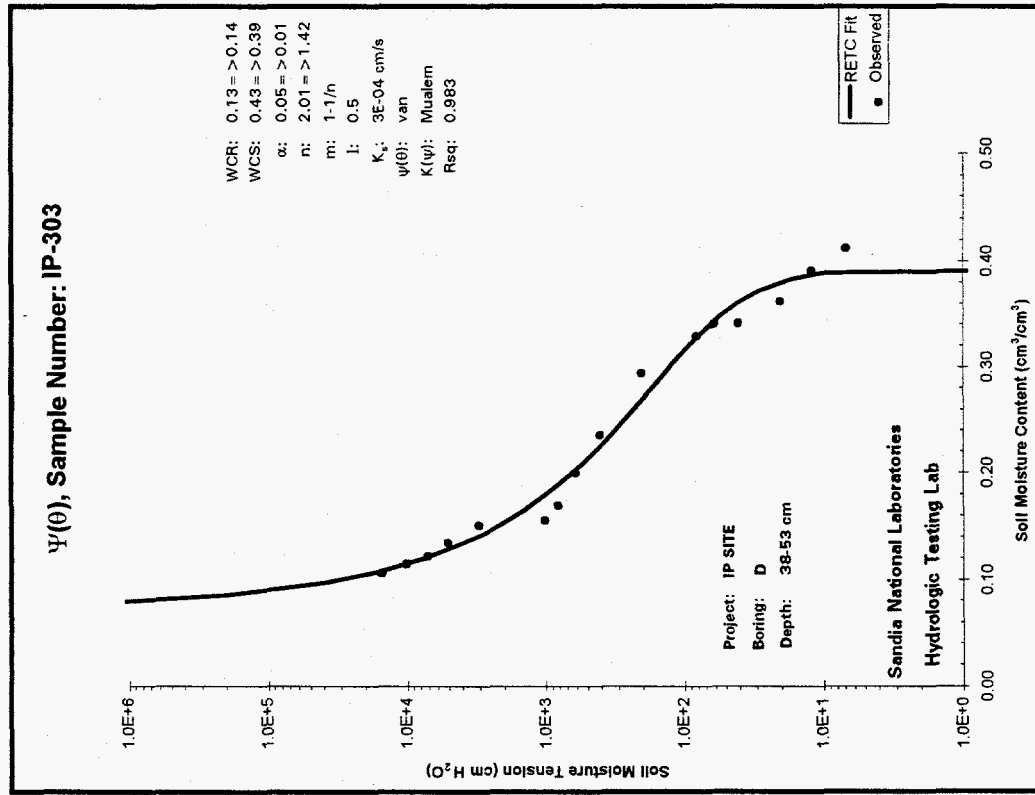
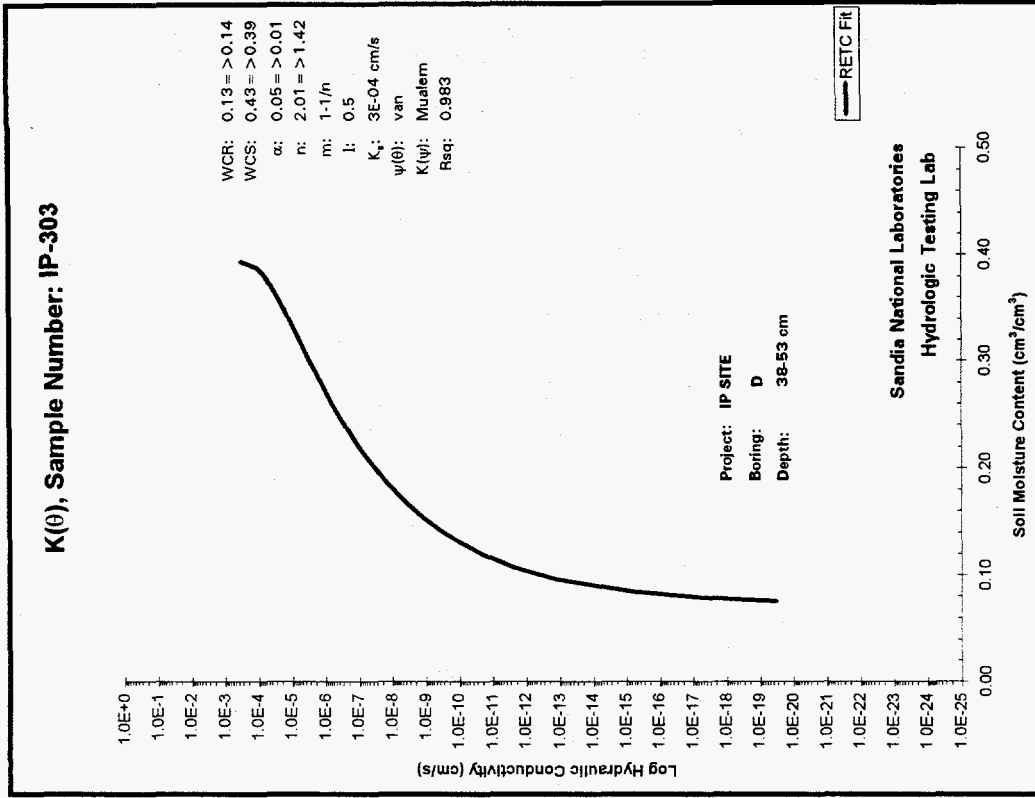


Figure A-4. RETC simulations of $\psi(\theta)$ and $K(\theta)$ relationships for the laboratory-tested sample from 38 - 53 cm bgs.

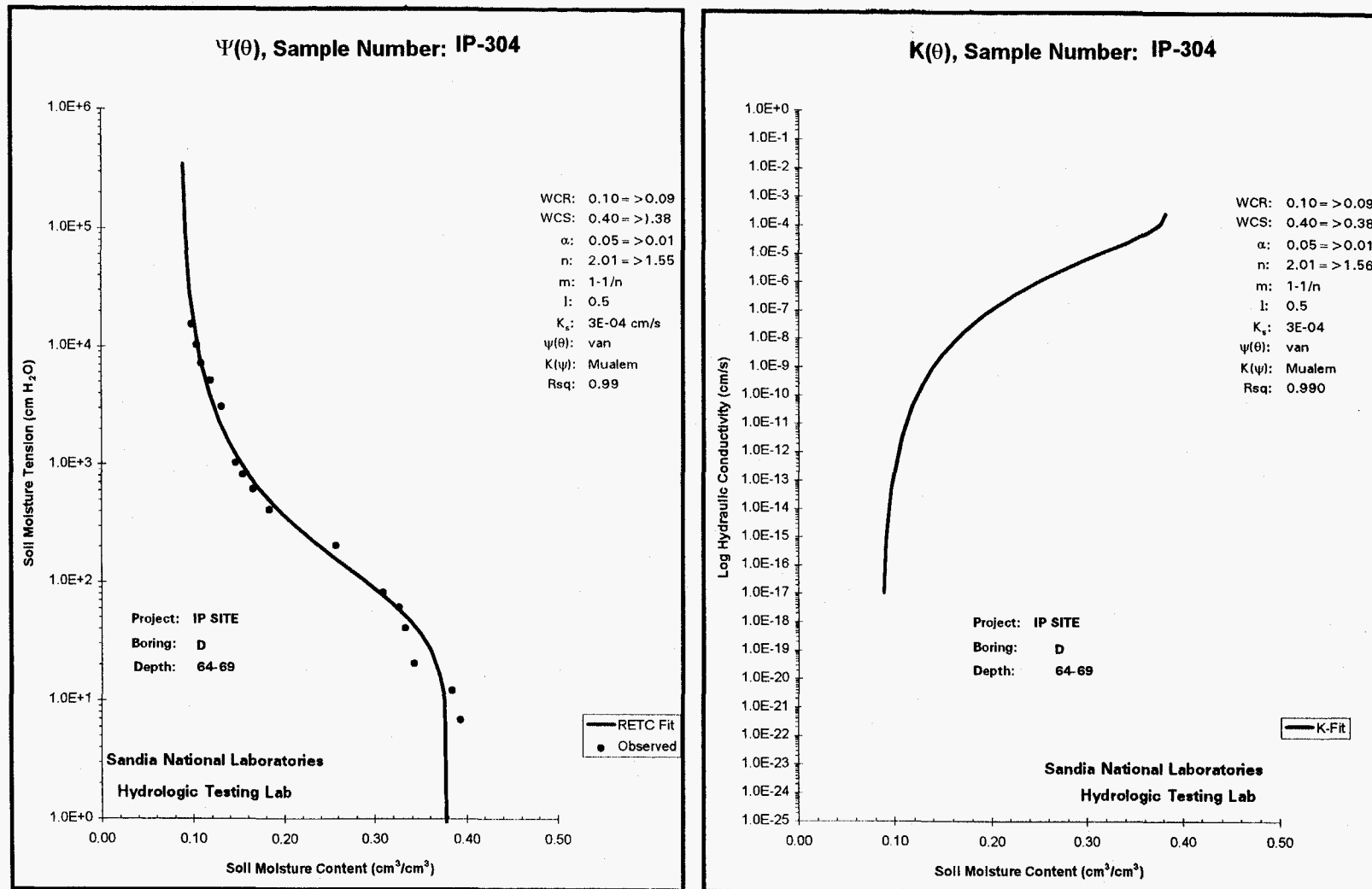


Figure A-5. RETC simulations of $\psi(\theta)$ and $K(\theta)$ relationships for the laboratory-tested sample from 64 - 69 cm bgs.

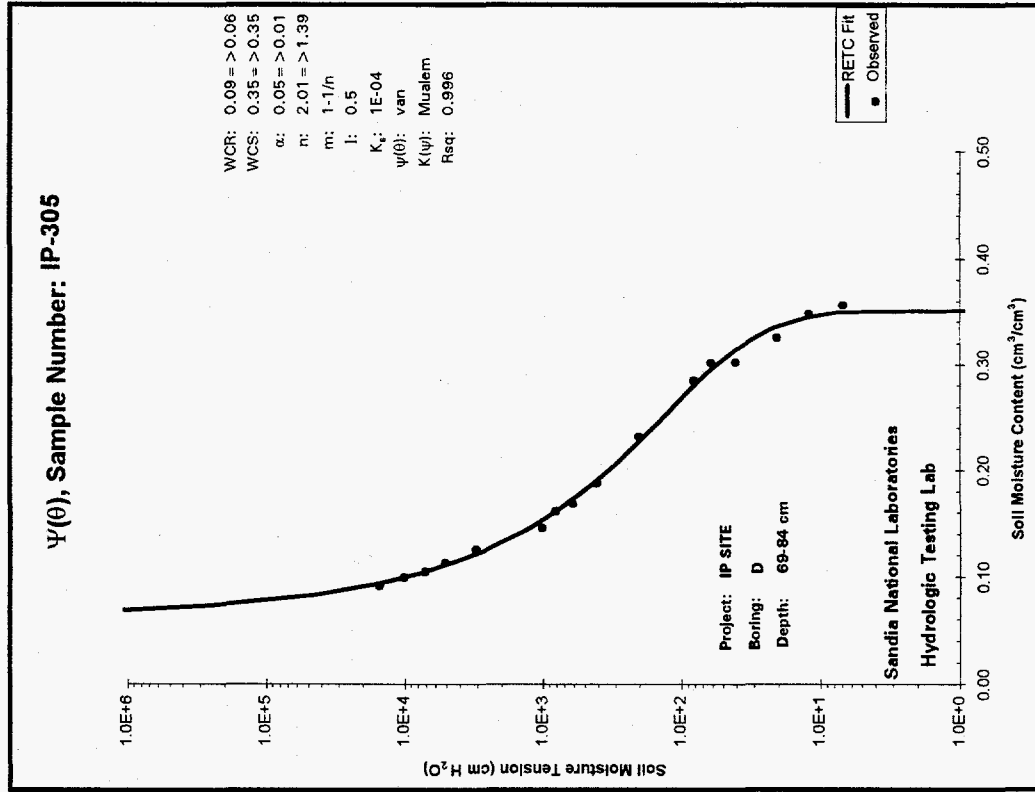
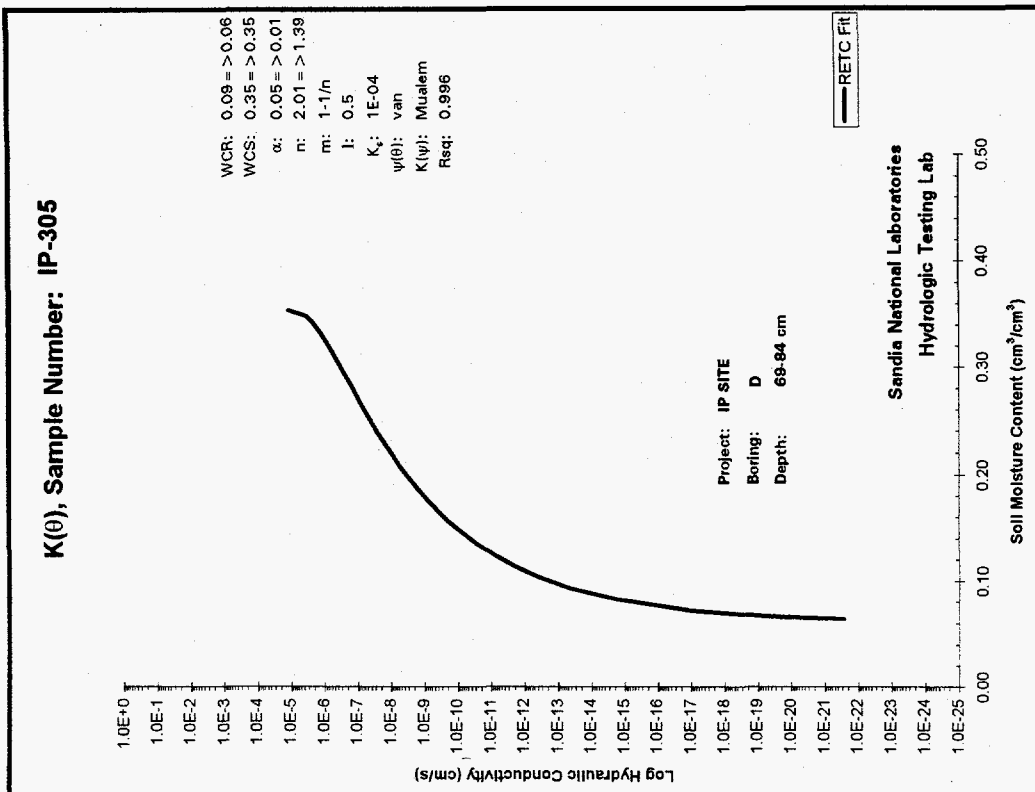


Figure A-6. RETC simulations of $\psi(\theta)$ and $K(\theta)$ relationships for the laboratory-tested sample from 69 - 84 cm bgs.

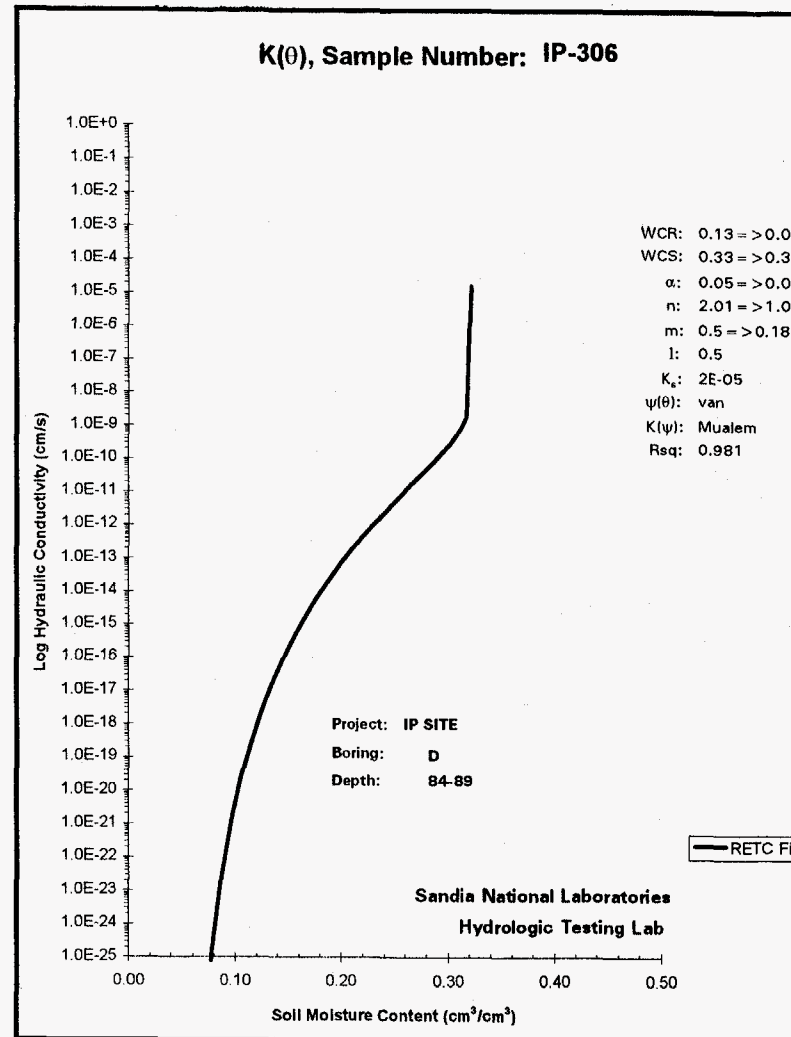
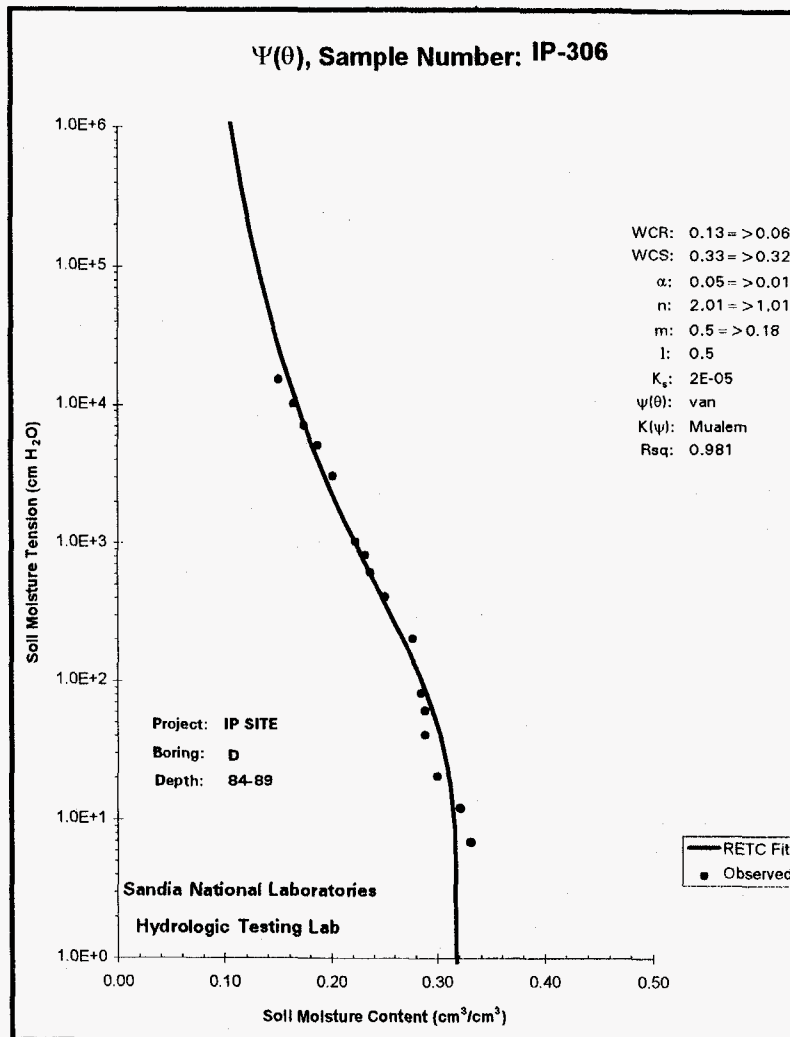


Figure A-7. RETC simulations of $\psi(\theta)$ and $K(\theta)$ relationships for the laboratory-tested sample from 84 - 89 cm bgs.

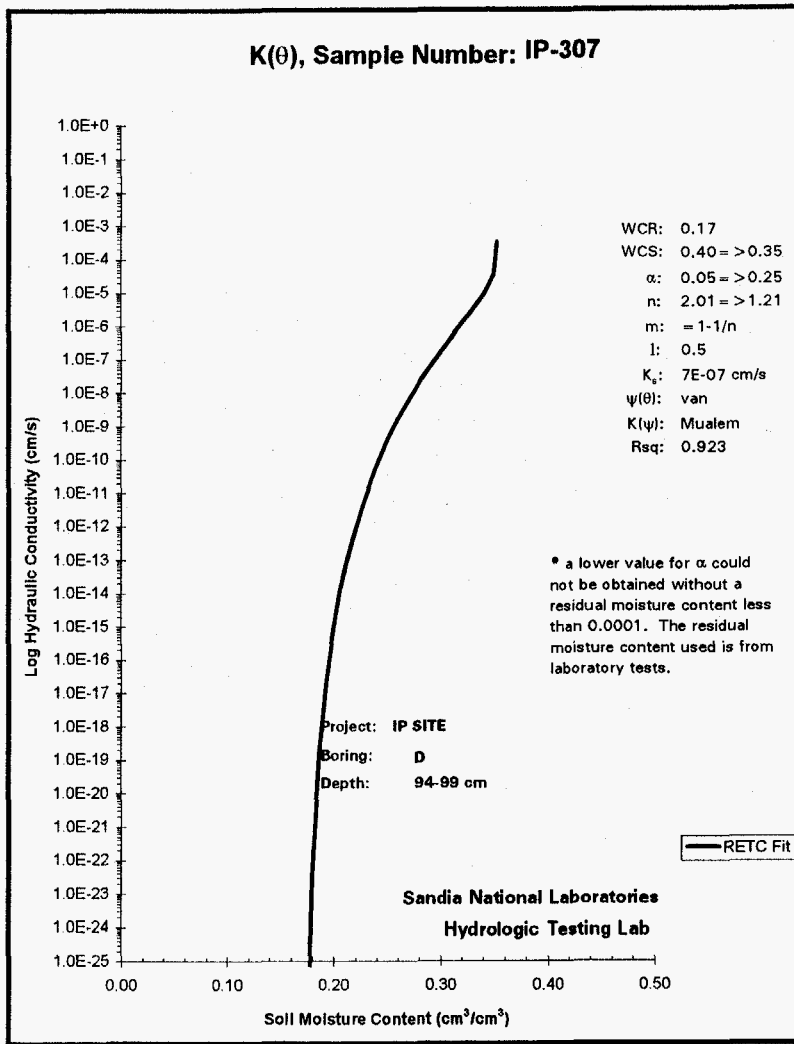
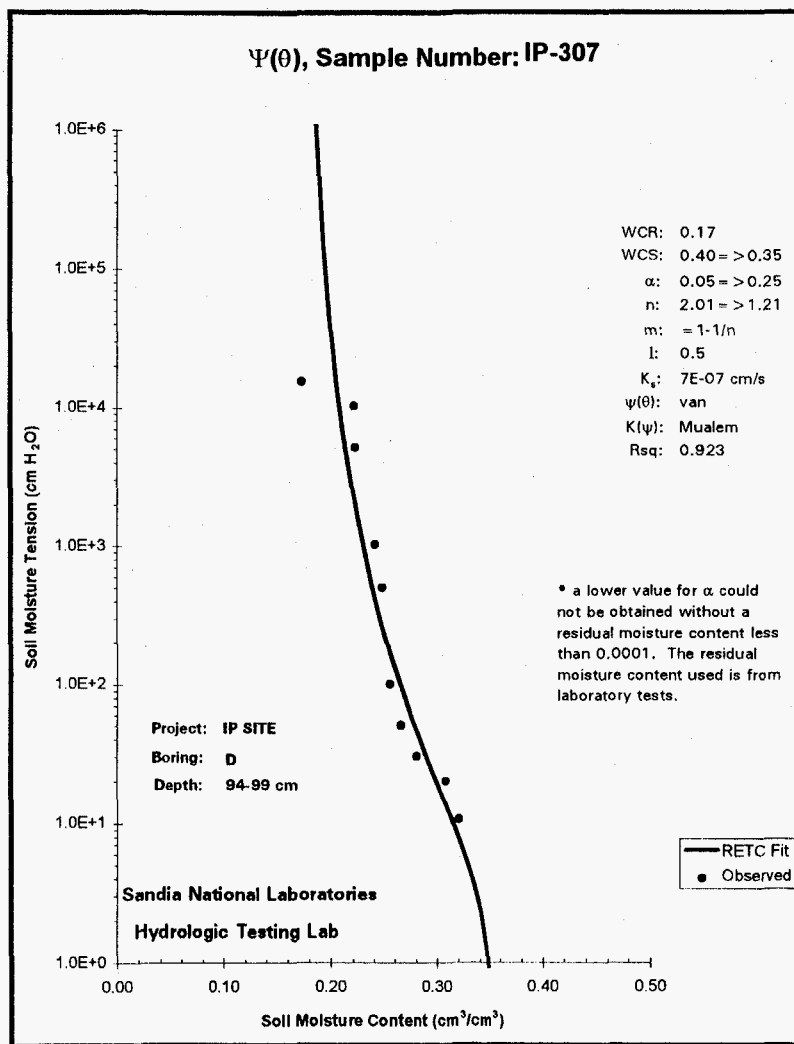


Figure A-8. RETC simulations of $\psi(\theta)$ and $K(\theta)$ relationships for the laboratory-tested sample from 94 - 97 cm bgs.

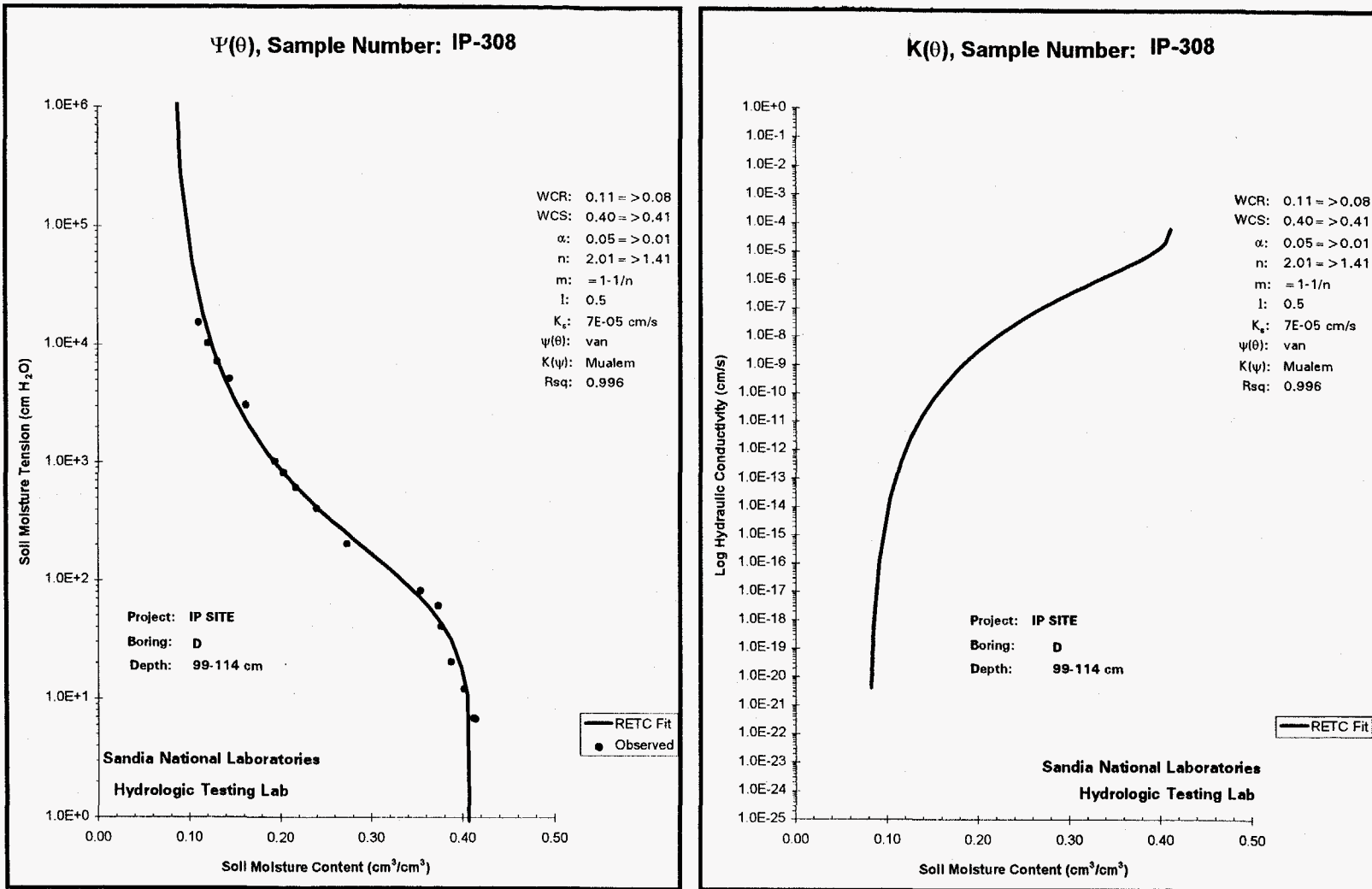


Figure A-9. RETC simulations of $\psi(\theta)$ and $K(\theta)$ relationships for the laboratory-tested sample from 99 - 114 cm bgs.

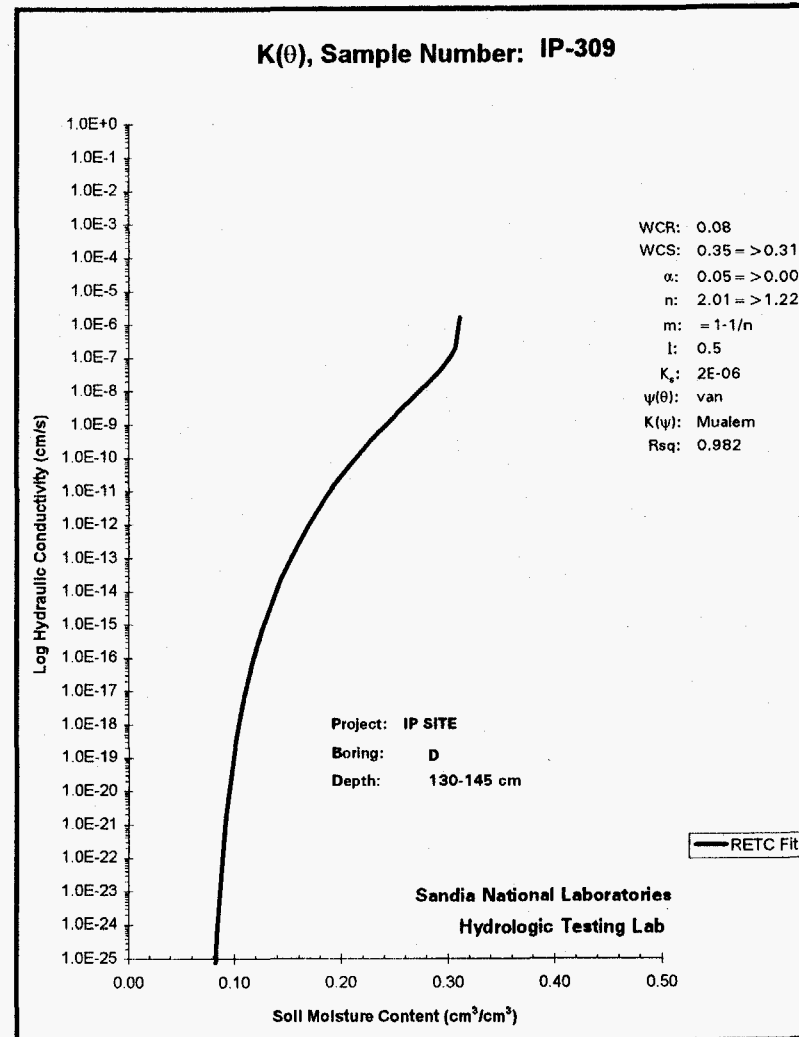
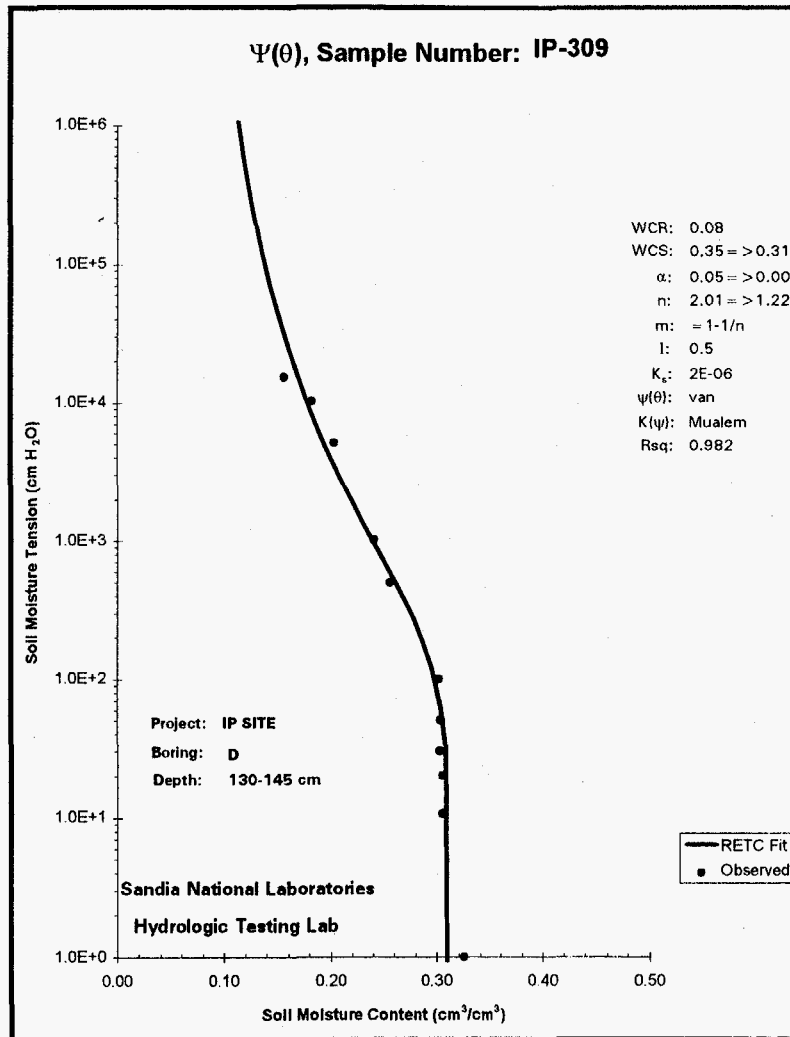


Figure A-10. RETC simulations of $\psi(\theta)$ and $K(\theta)$ relationships for the laboratory-tested sample from 130 - 145 cm bgs.

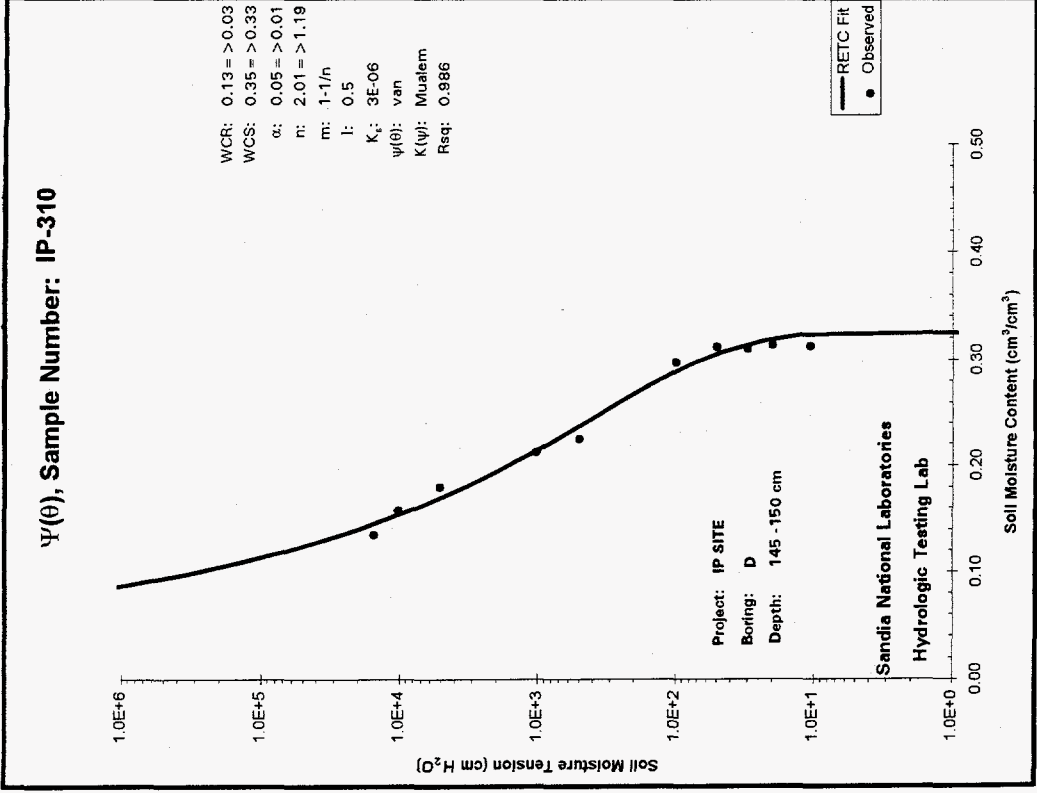
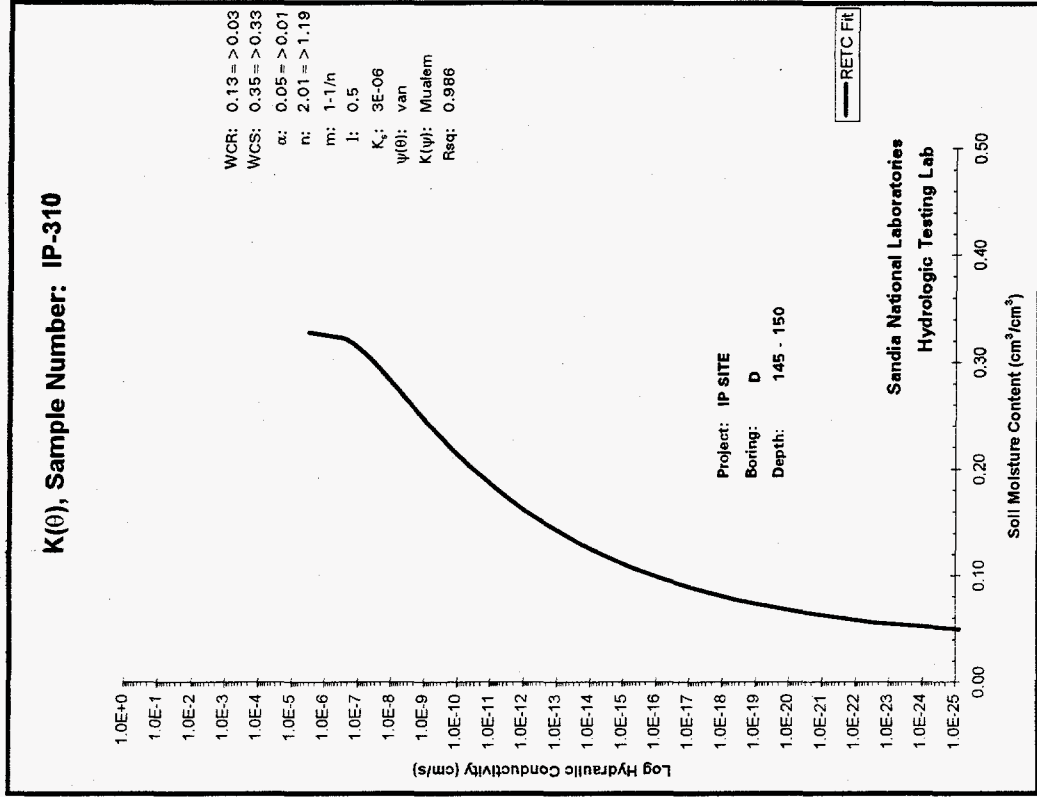


Figure A-11. RETC simulations of $\psi(\theta)$ and $K(\theta)$ relationships for the laboratory-tested sample from 145 - 150 cm bgs.

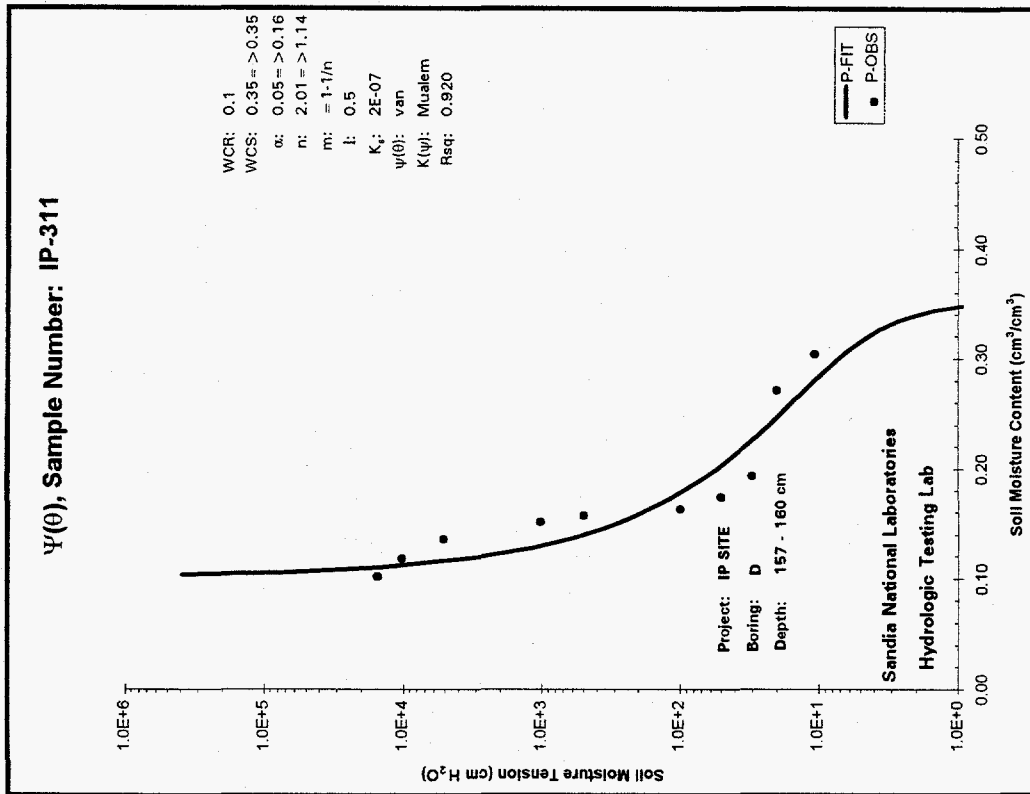
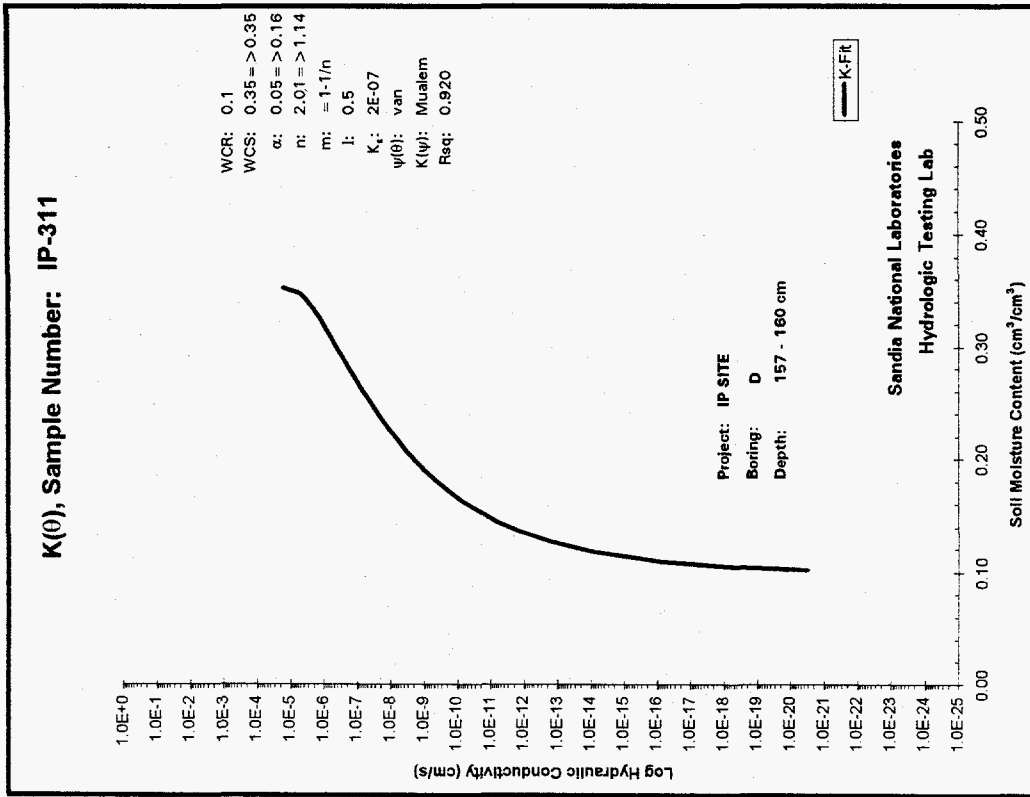


Figure A-12. RETC simulations of $\psi(\theta)$ and $K(\theta)$ relationships for the laboratory-tested sample from 157 - 160 cm bgs.

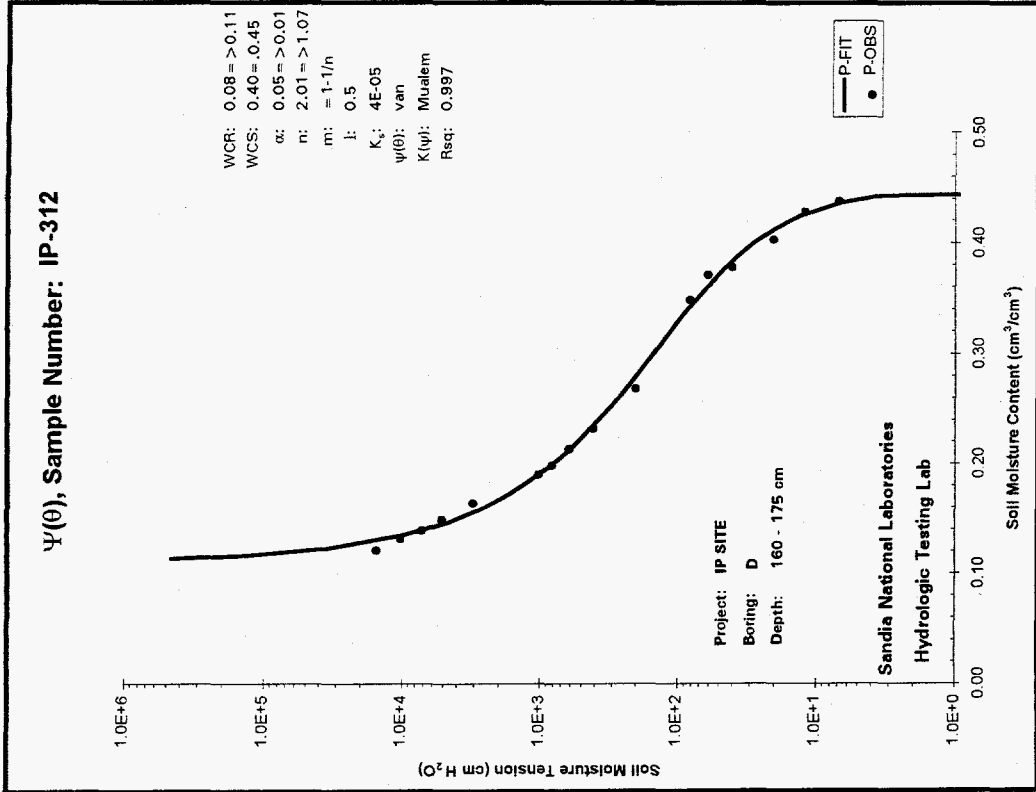
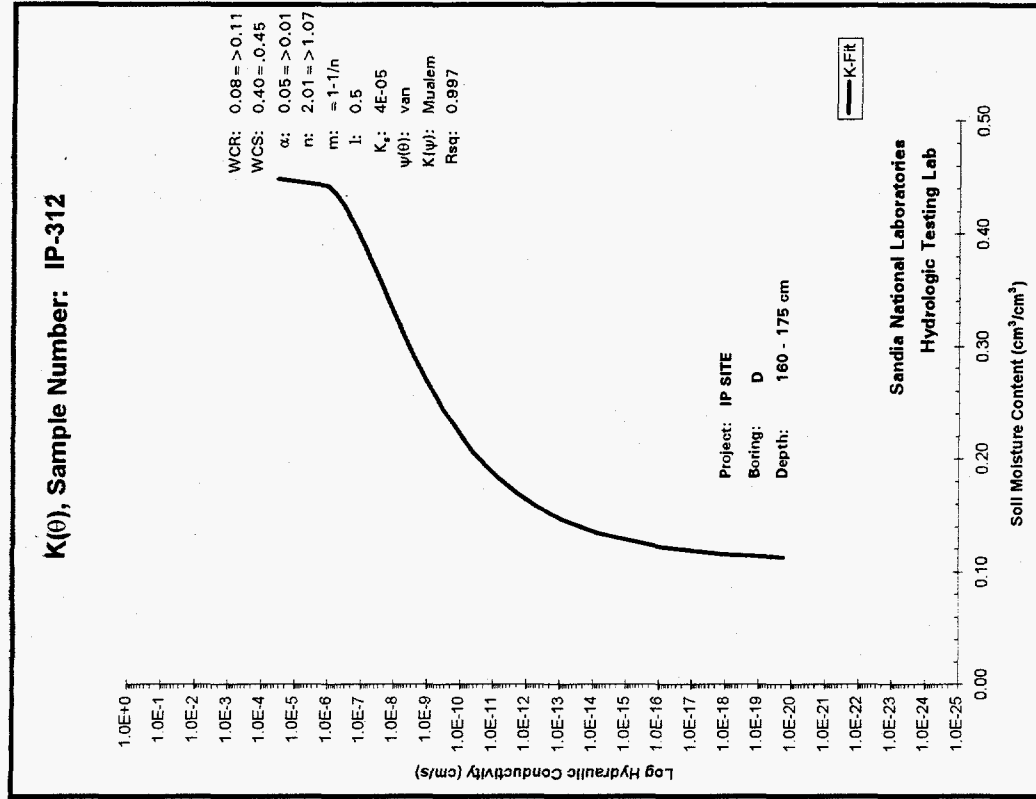


Figure A-13. RETC simulations of $\psi(\theta)$ and $K(\theta)$ relationships for the laboratory-tested sample from 160 - 175 cm bgs.

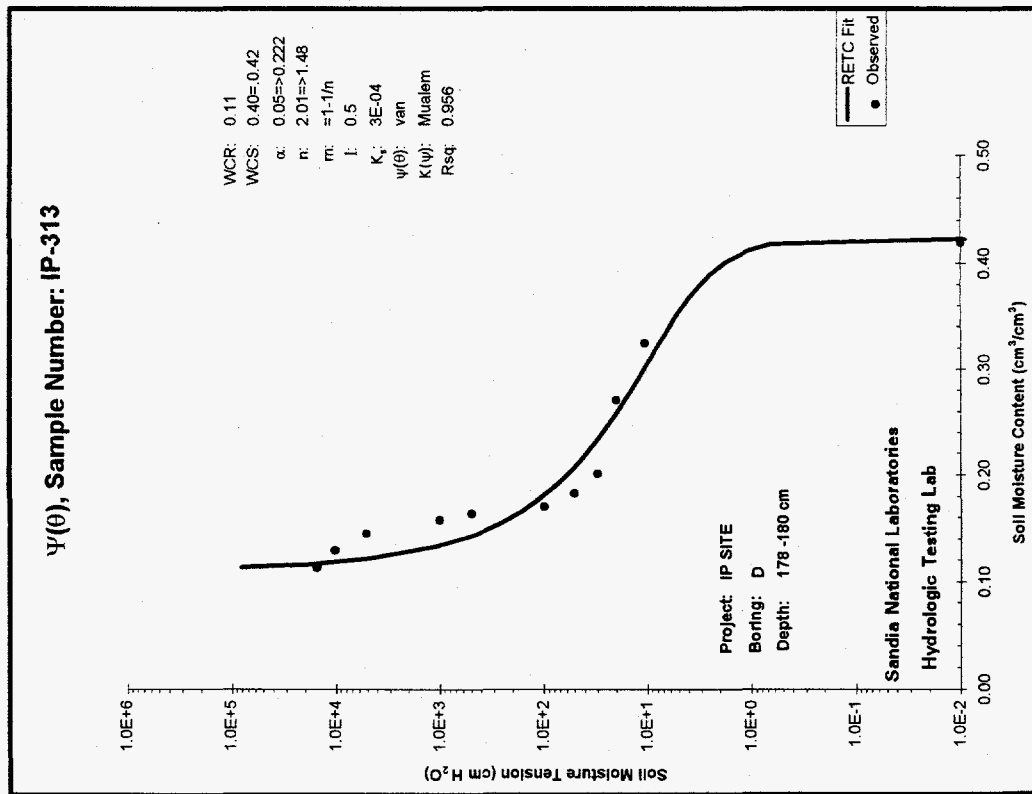
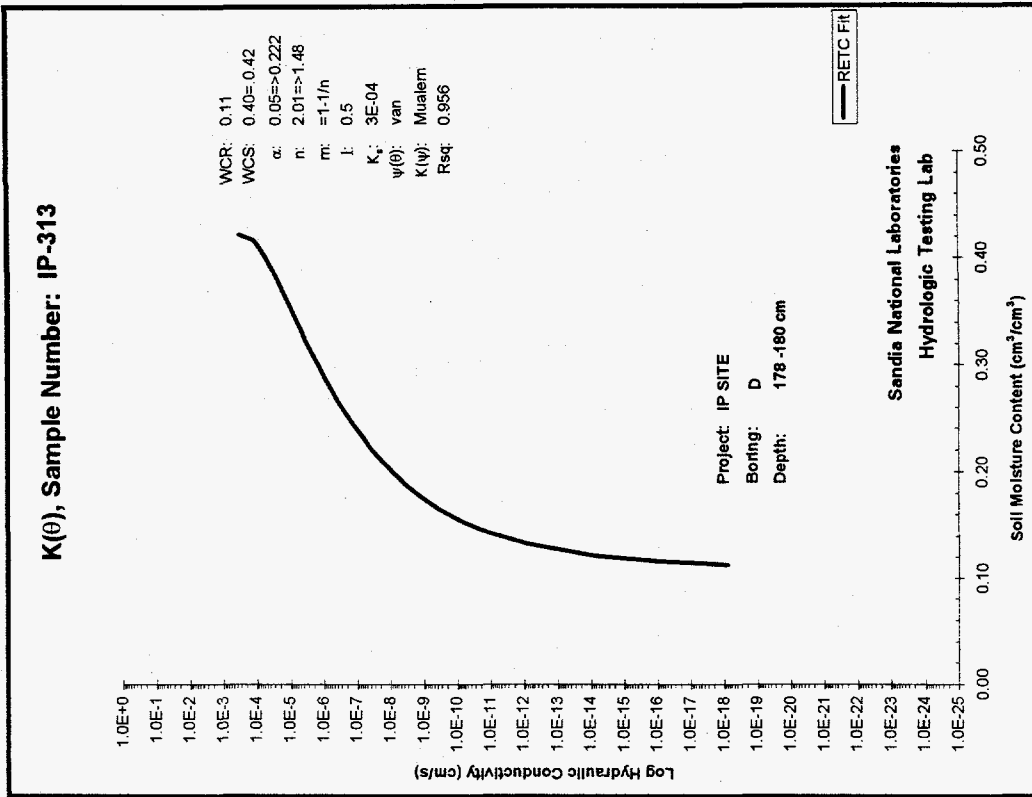


Figure A-14. RETC simulations of $\psi(\theta)$ and $K(\theta)$ relationships for the laboratory-tested sample from 178-180 cm bgs.

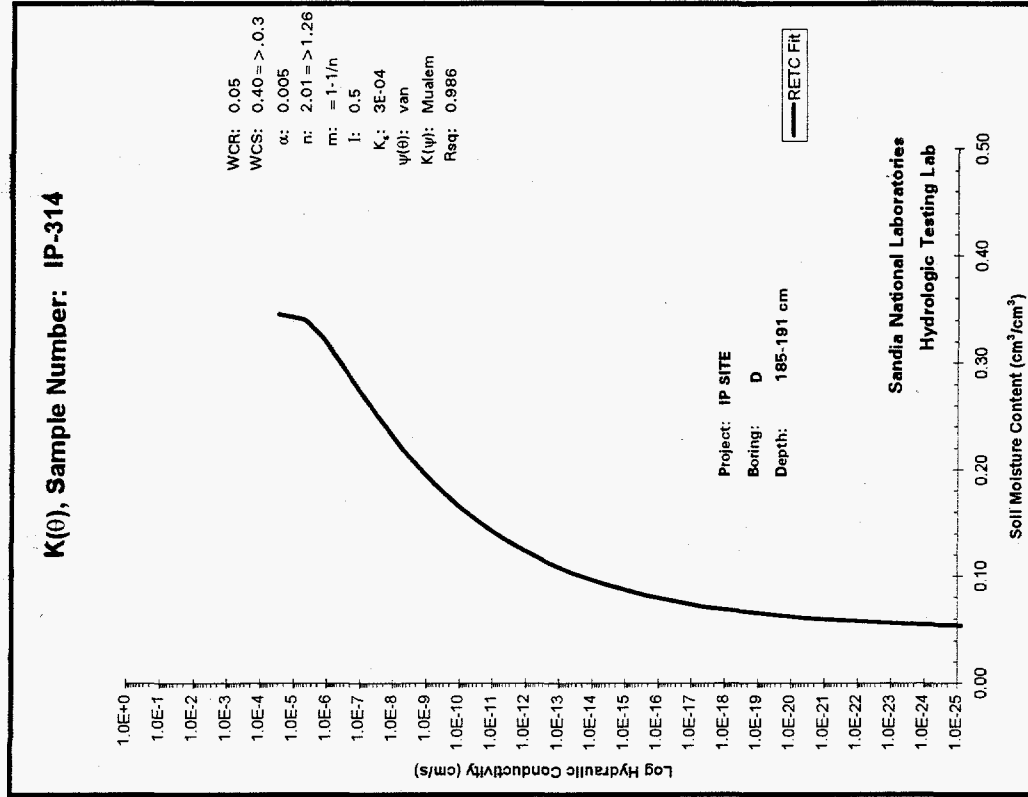
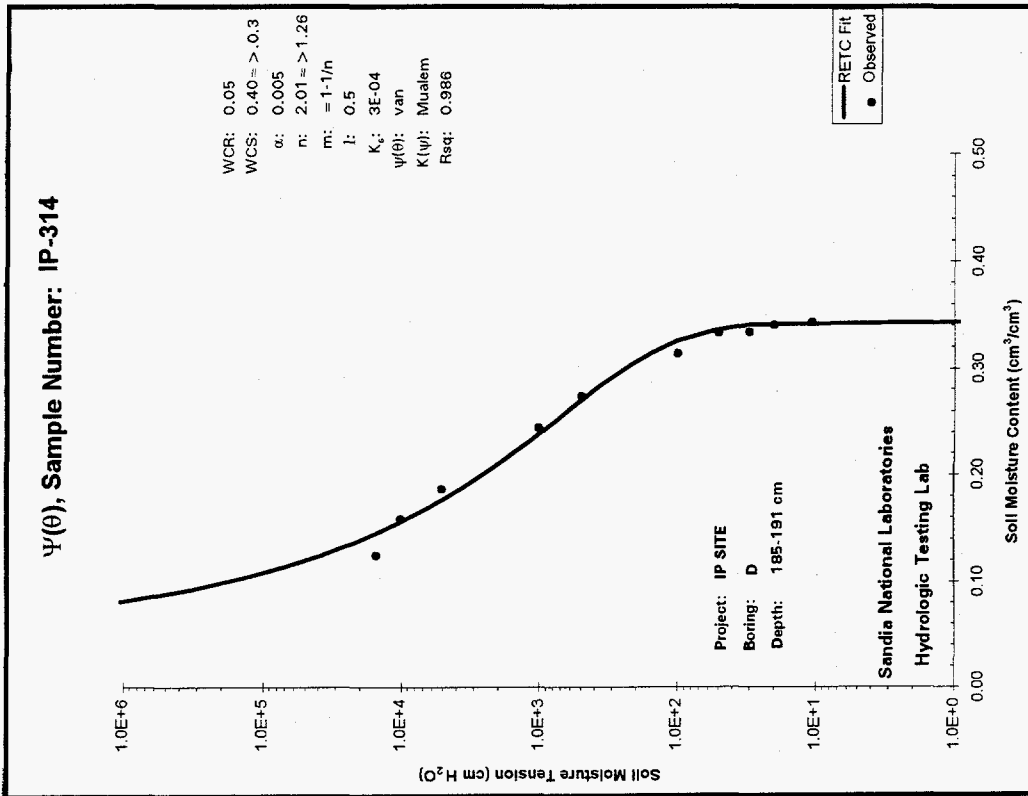


Figure A-15. RETC simulations of $\psi(\theta)$ and $K(\theta)$ relationships for the laboratory-tested sample from 185 - 191 cm bgs.

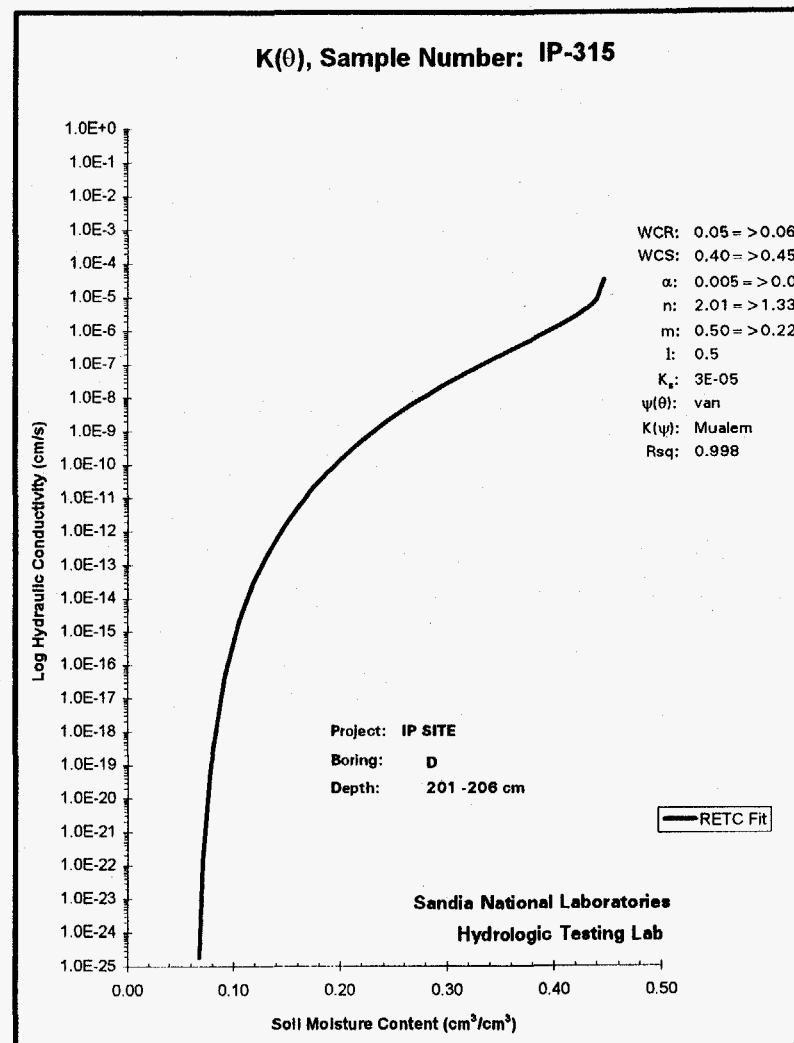
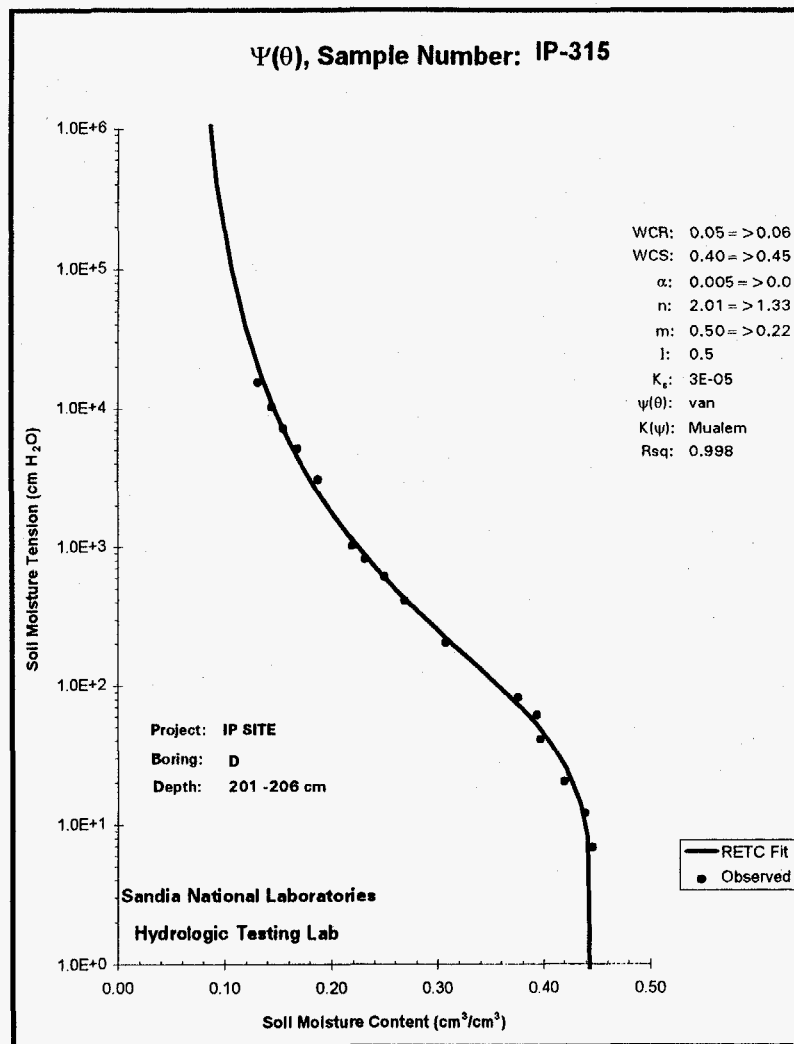


Figure A-16. RETC simulations of $\psi(\theta)$ and $K(\theta)$ relationships for the laboratory-tested sample from 201 - 206 cm bgs.

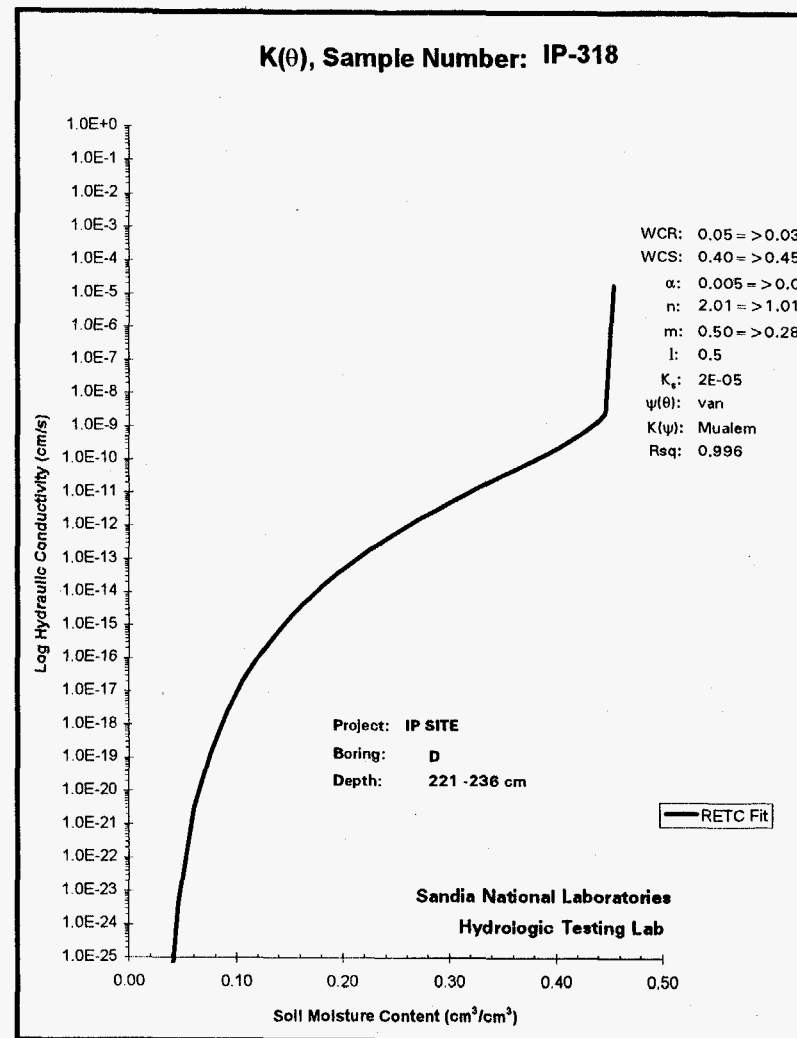
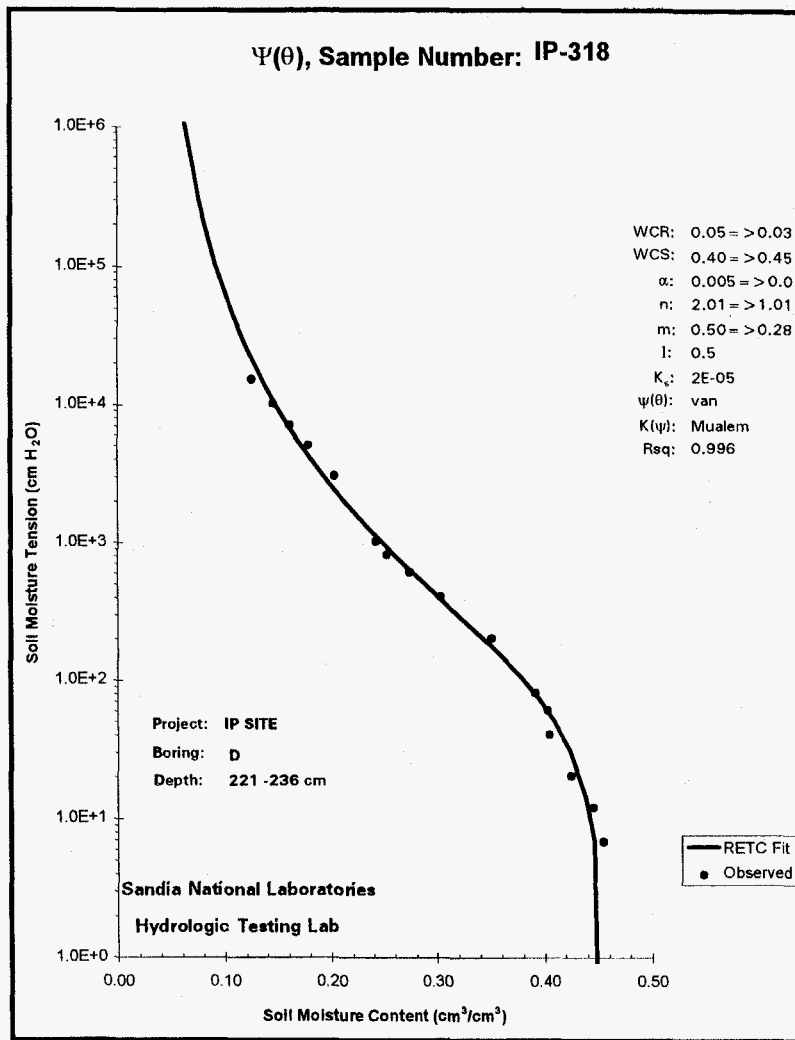


Figure A-17. RETC simulations of $\psi(\theta)$ and $K(\theta)$ relationships for the laboratory-tested sample from 221 - 236 cm bgs.

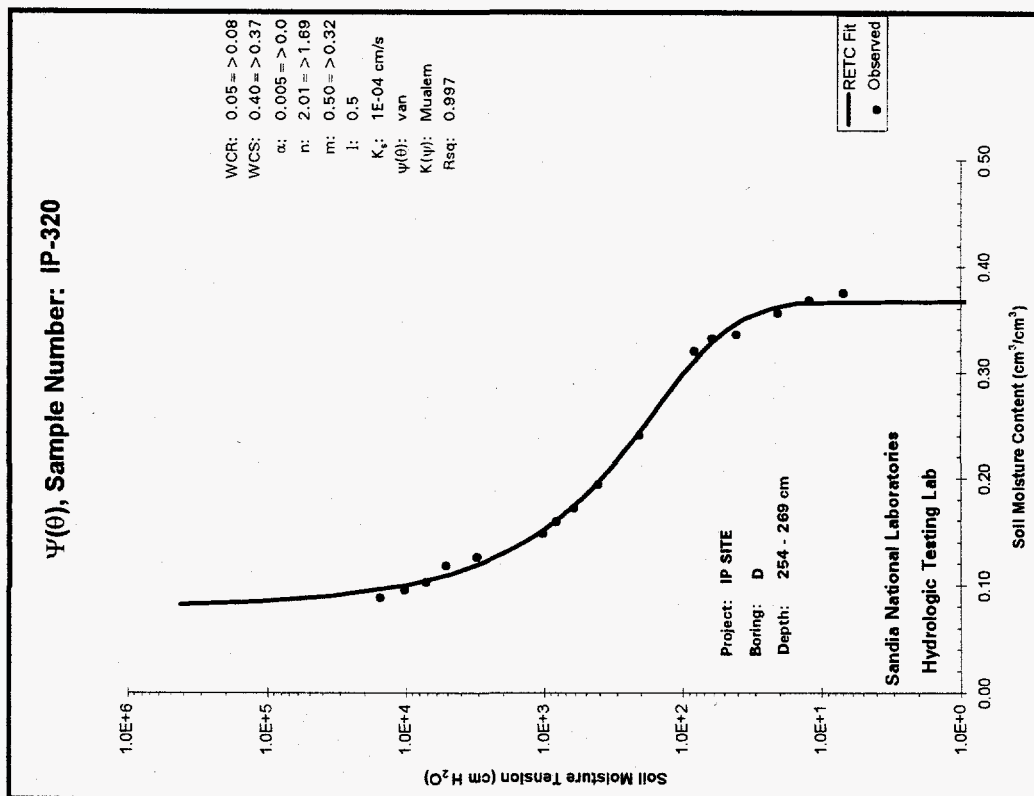
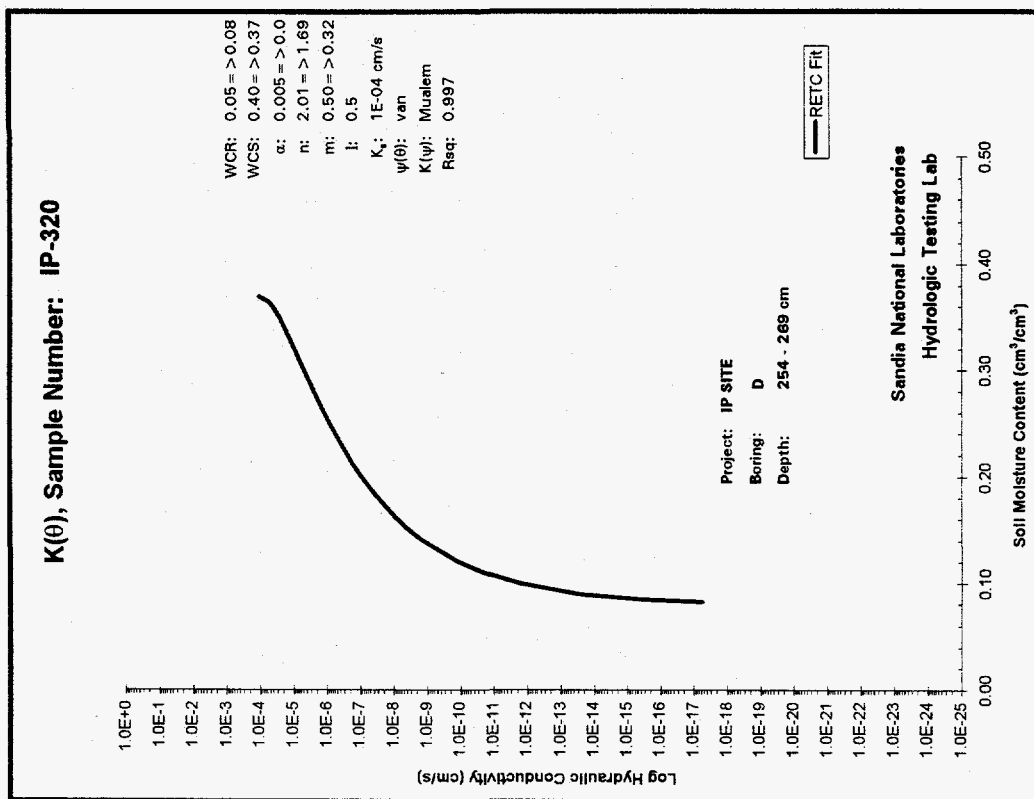


Figure A-18. RETC simulations of $\psi(\theta)$ and $K(\theta)$ relationships for the laboratory-tested sample from 254 - 269 cm bgs.

Section 2.0 Graphs of RETC predictions of unsaturated hydraulic conductivity based on data from field infiltration results

Section 2.0 present the results of RETC modeling of the $K(\theta)$ relationship based solely on data obtained during and after the infiltration event of the IP test. Results are presented beginning at the 15 to 45 cm interval bgs and ending with the 165 to 195 cm bgs interval.

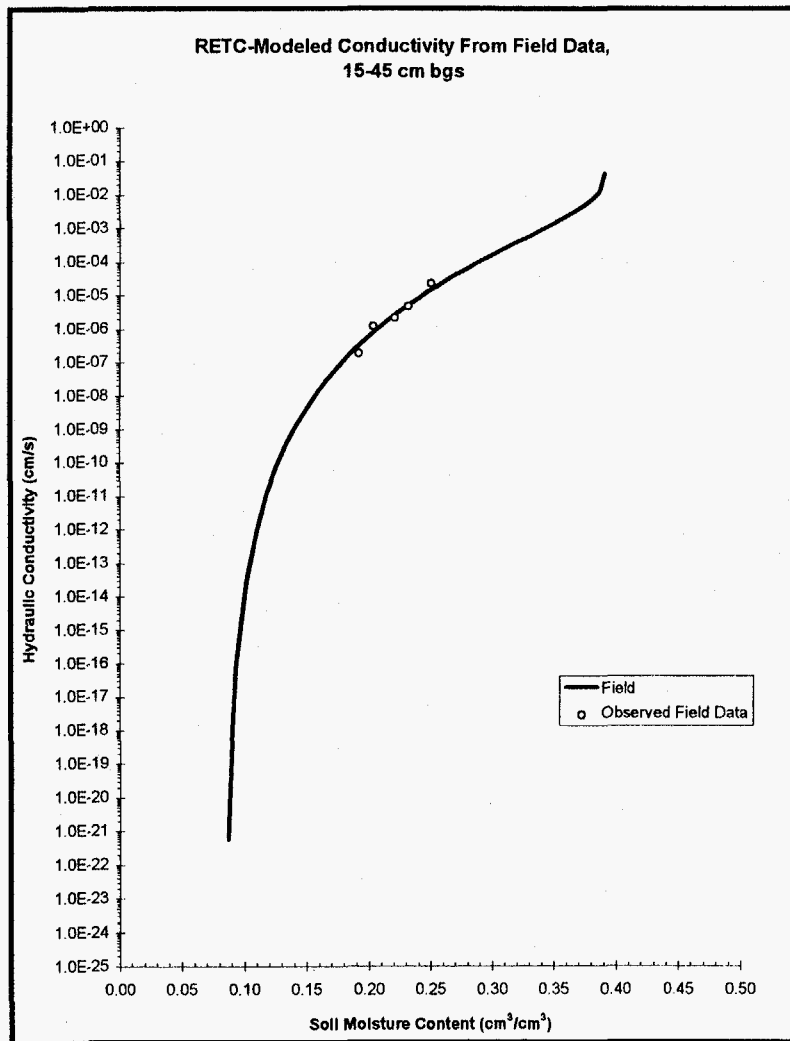


Figure A2-1. RETC prediction of $K(\theta)$ from IP data at 15 - 45 cm bgs.

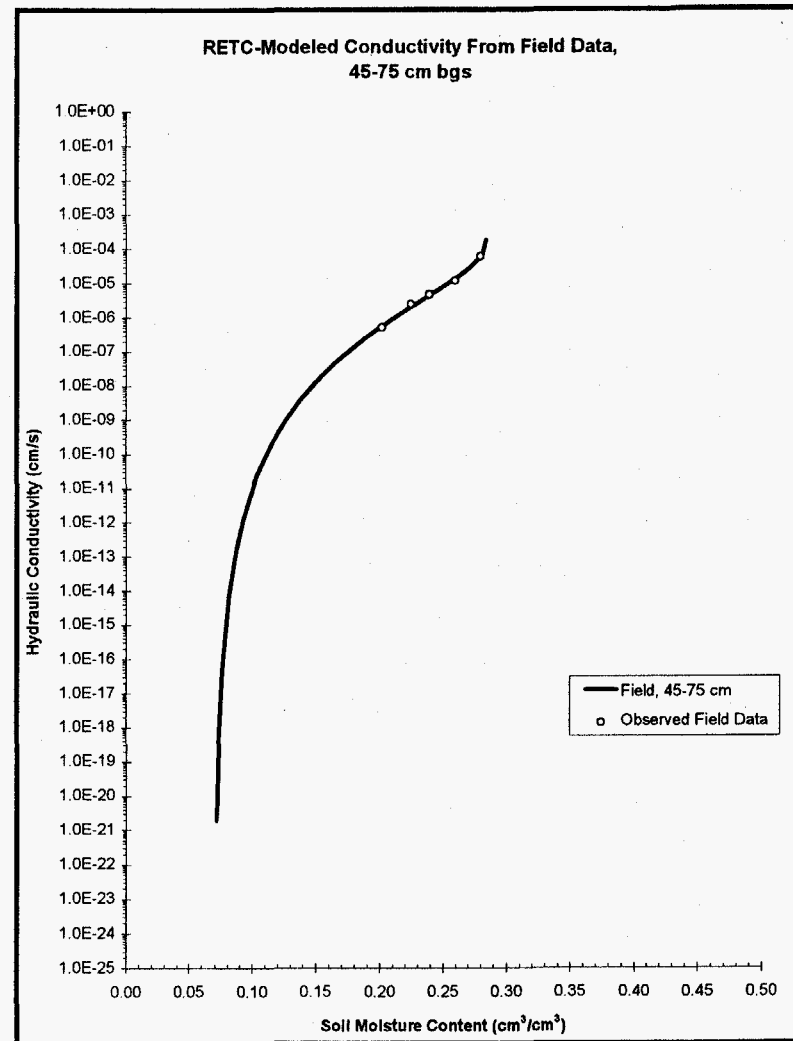


Figure A2-2. RETC predictions of $K(\theta)$ from IP data at 45 - 75 cm bgs

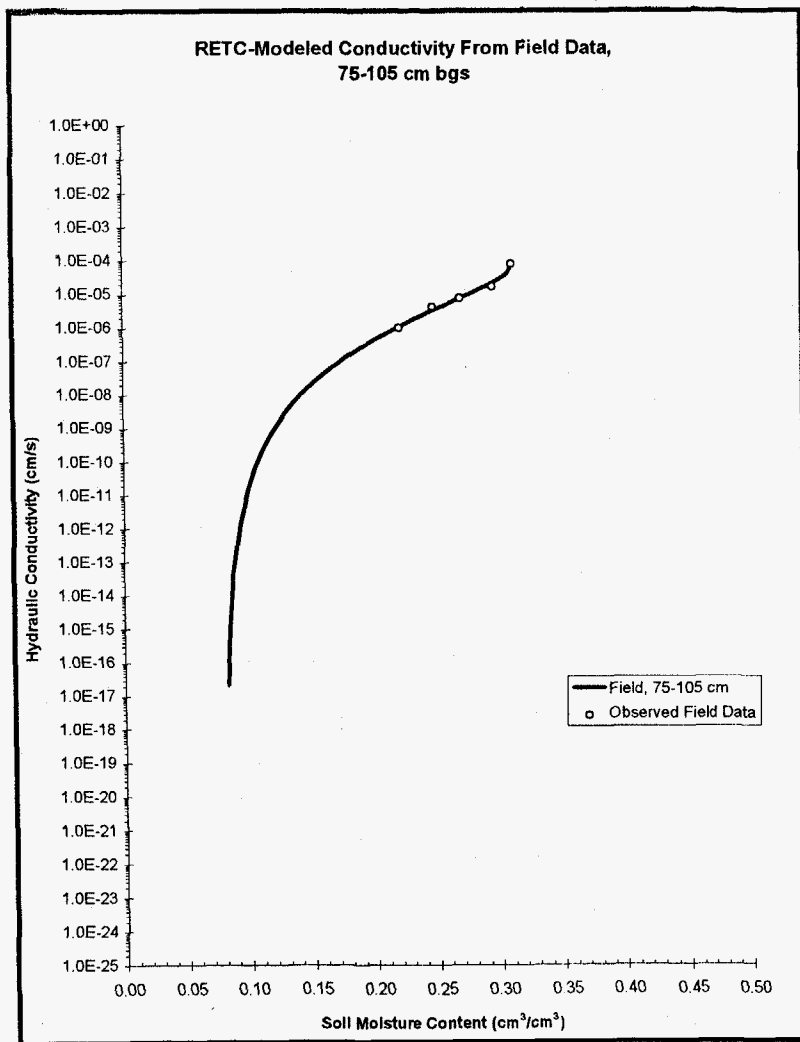


Figure A2-3. RETC prediction of $K(\theta)$ from IP data
at 75 - 105 cm bgs.

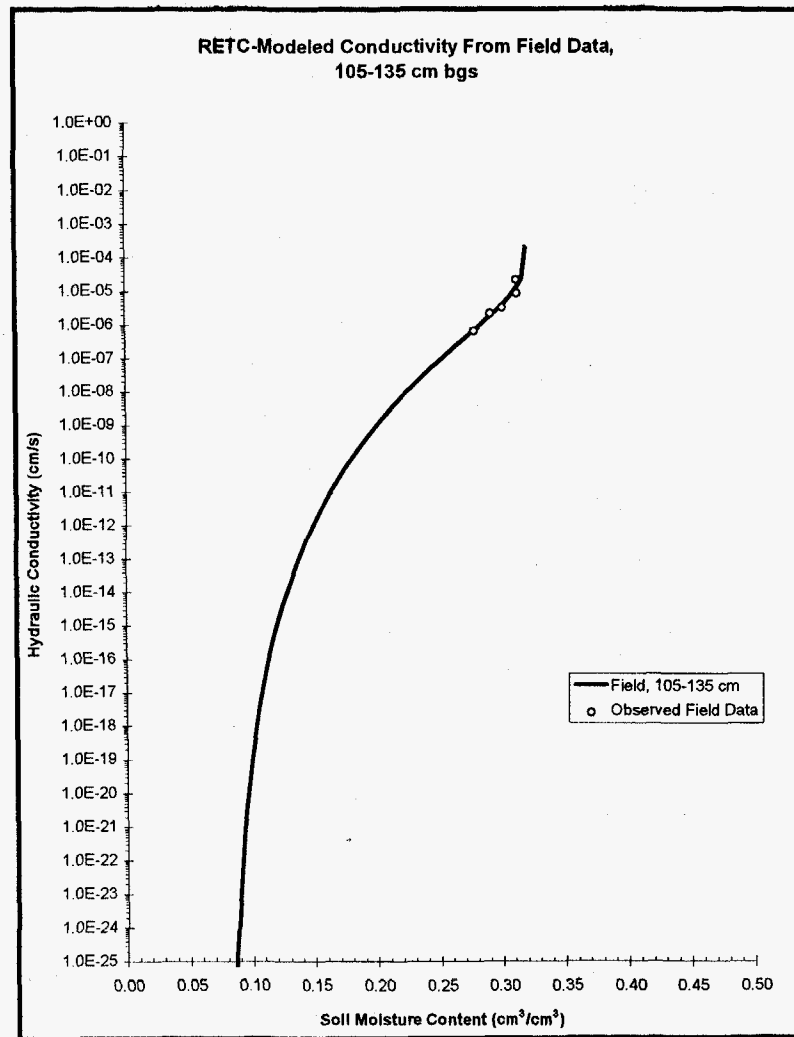


Figure A2-4. RETC prediction of $K(\theta)$ from IP data
at 105 - 135 cm bgs

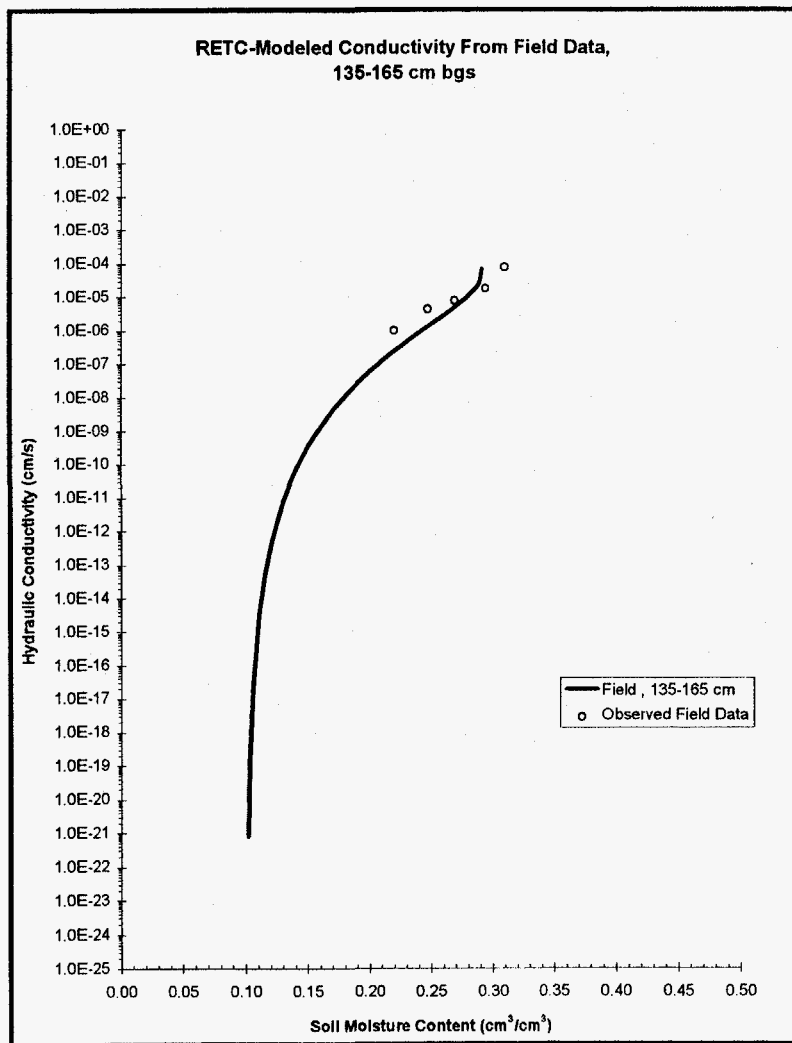


Figure A2-5. RETC prediction of $K(\theta)$ from IP data at 135 - 165 cm bgs.

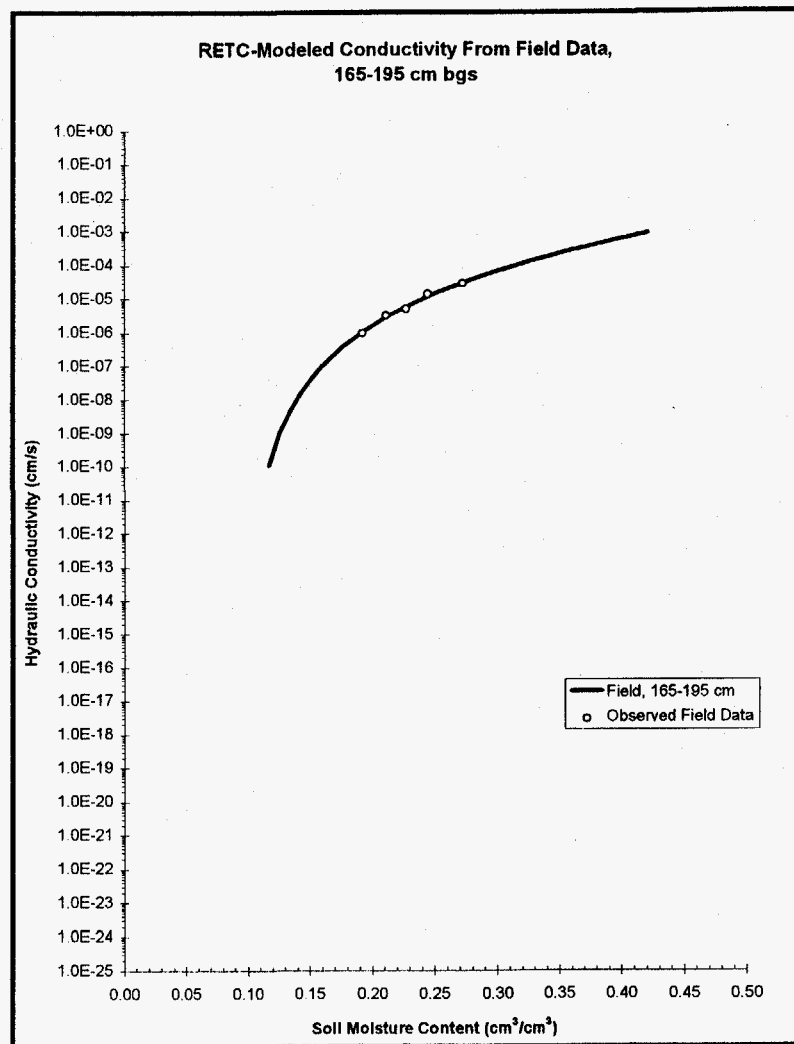


Figure A2-6. RETC prediction of $K(\theta)$ from field (IP) data at 165 - 195 cm bgs.

Section 3.0 Graphs of RETC predictions of unsaturated hydraulic conductivity from data sets combining both lab and IP data

Section 3.0 contains graphs of RETC predictions of the unsaturated hydraulic conductivity based on laboratory-tested $\psi(\theta)$ data combined with $K(\theta)$ data from the IP test. Results are presented for 30 cm intervals beginning at 15 cm bgs and ending at 195 cm bgs.

For comparative and illustrative purposes, the $K(\theta)$ relationships for lab and IP data sets alone are also shown.

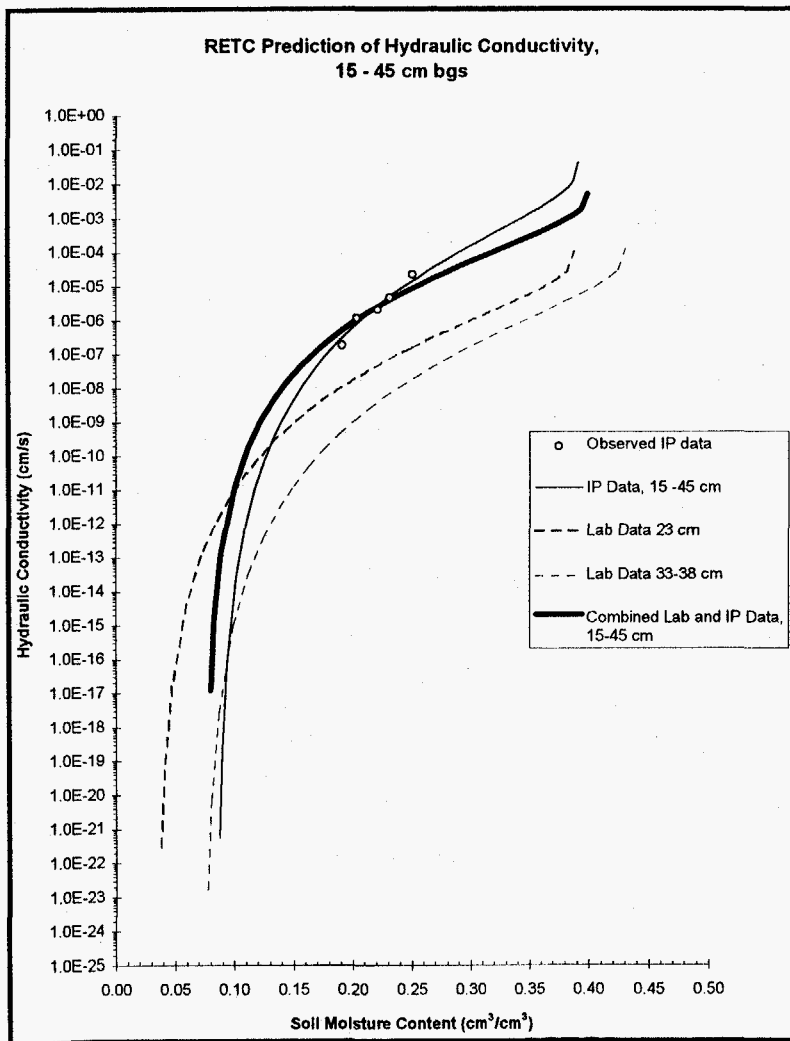


Figure A3-1. RETC-predicted $K(\theta)$ relationships from IP, laboratory, and combined laboratory and IP data, 15 - 45 cm bgs.

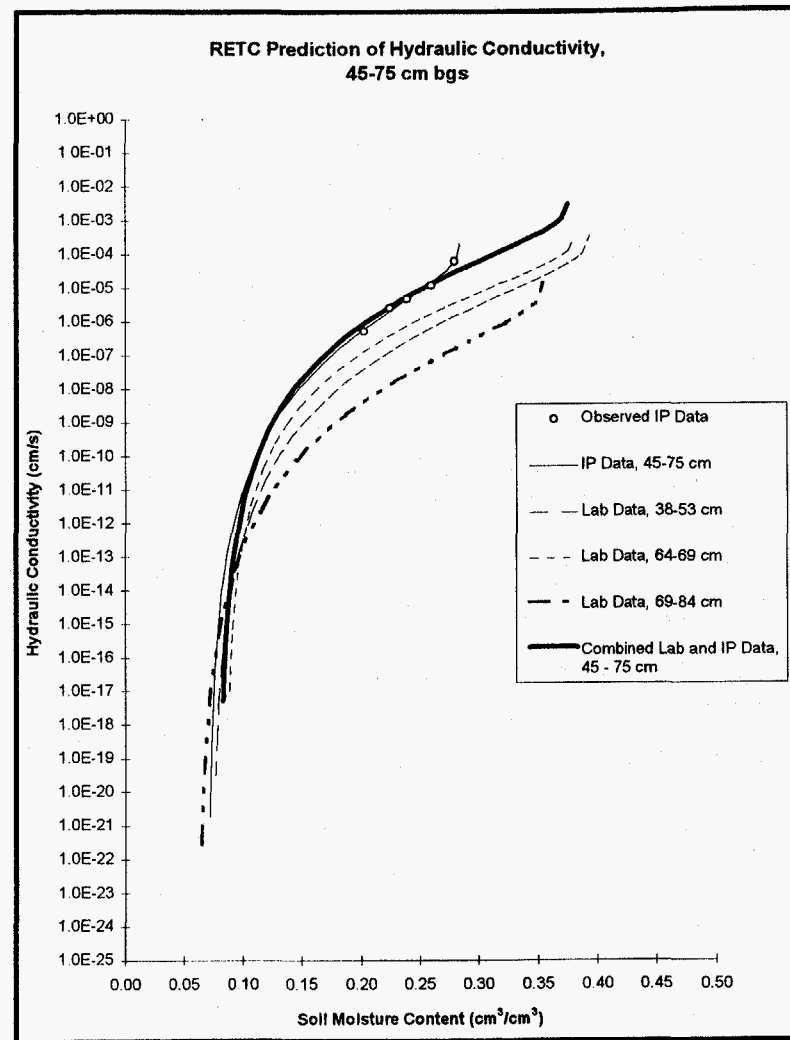


Figure A3-2. RETC-predicted $K(\theta)$ relationships from IP, laboratory, and combined laboratory and IP data, 45 - 75 cm bgs.

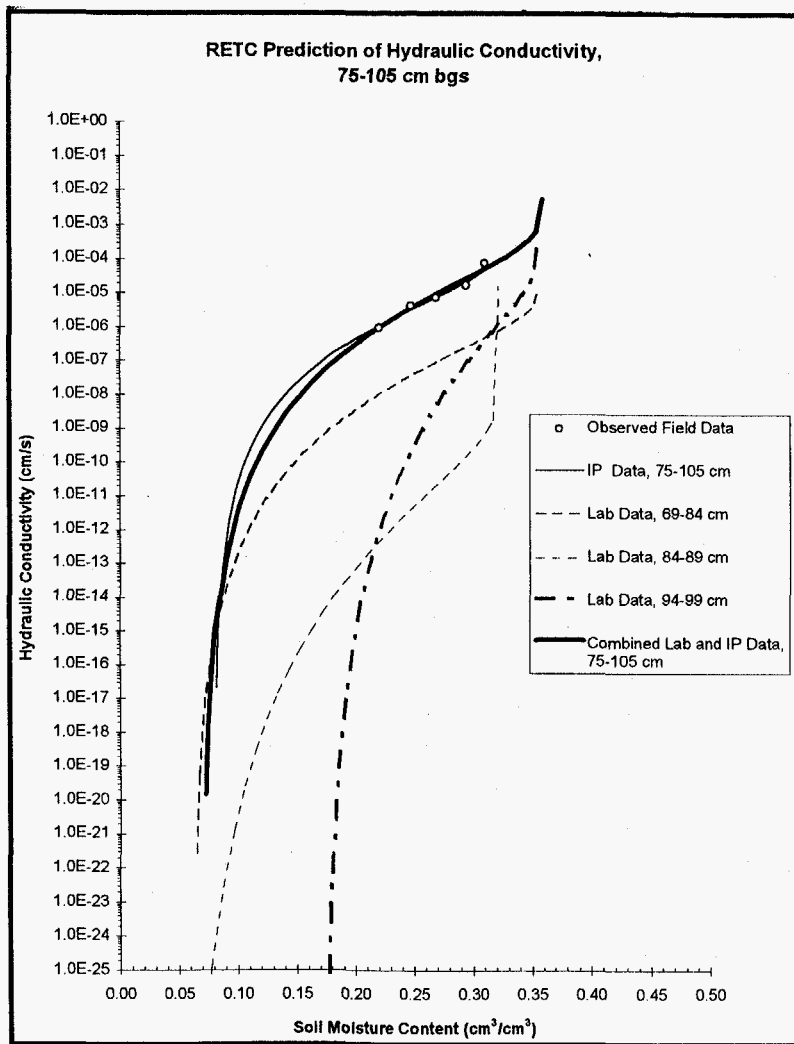


Figure A3-3. RETC-predicted $K(\theta)$ relationships from IP, laboratory, and combined laboratory and IP data, 75 - 105 cm bgs.

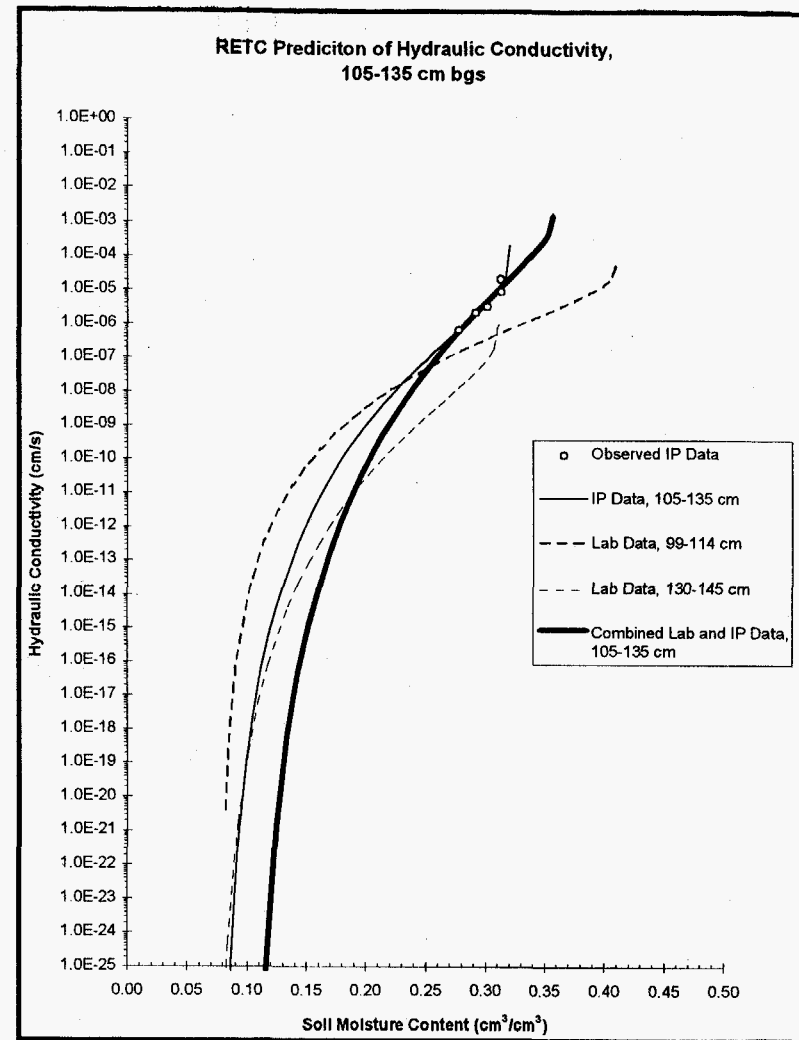


Figure A3-4. RETC-predicted $K(\theta)$ relationships from IP, laboratory, and combined laboratory and IP data, 105 - 135 cm bgs.

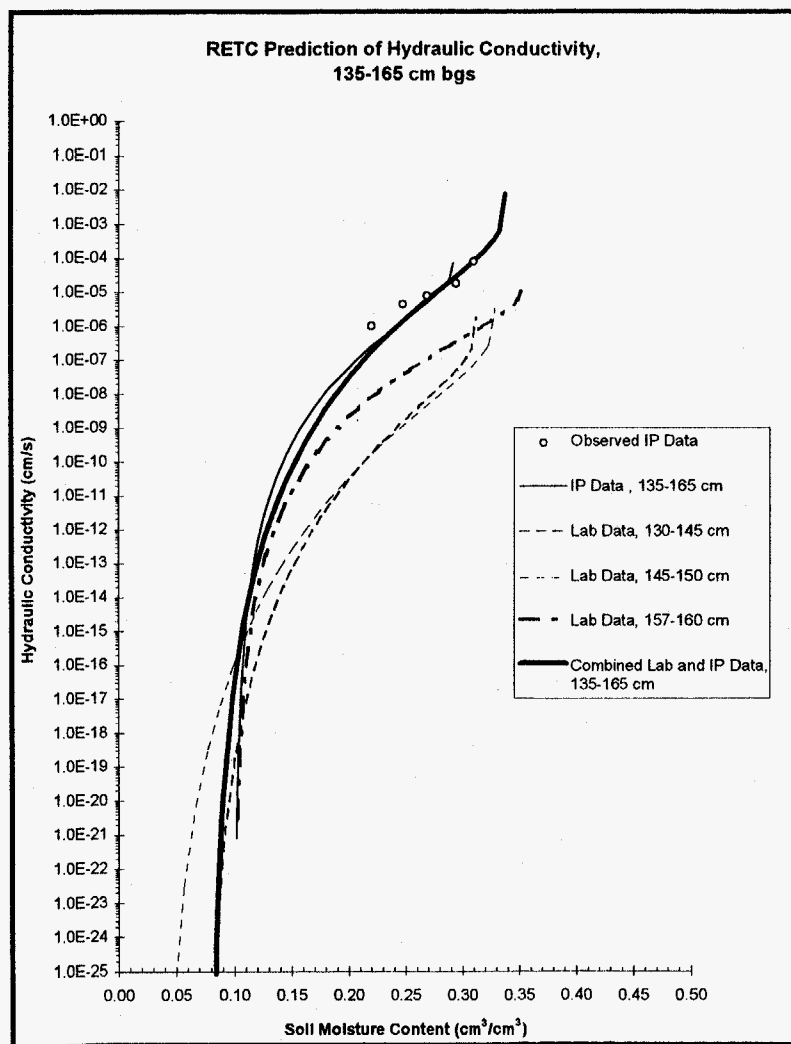


Figure A3-5. RETC-predicted $K(\theta)$ relationships from IP, laboratory, and combined laboratory and IP data, 135 - 165 cm bgs.

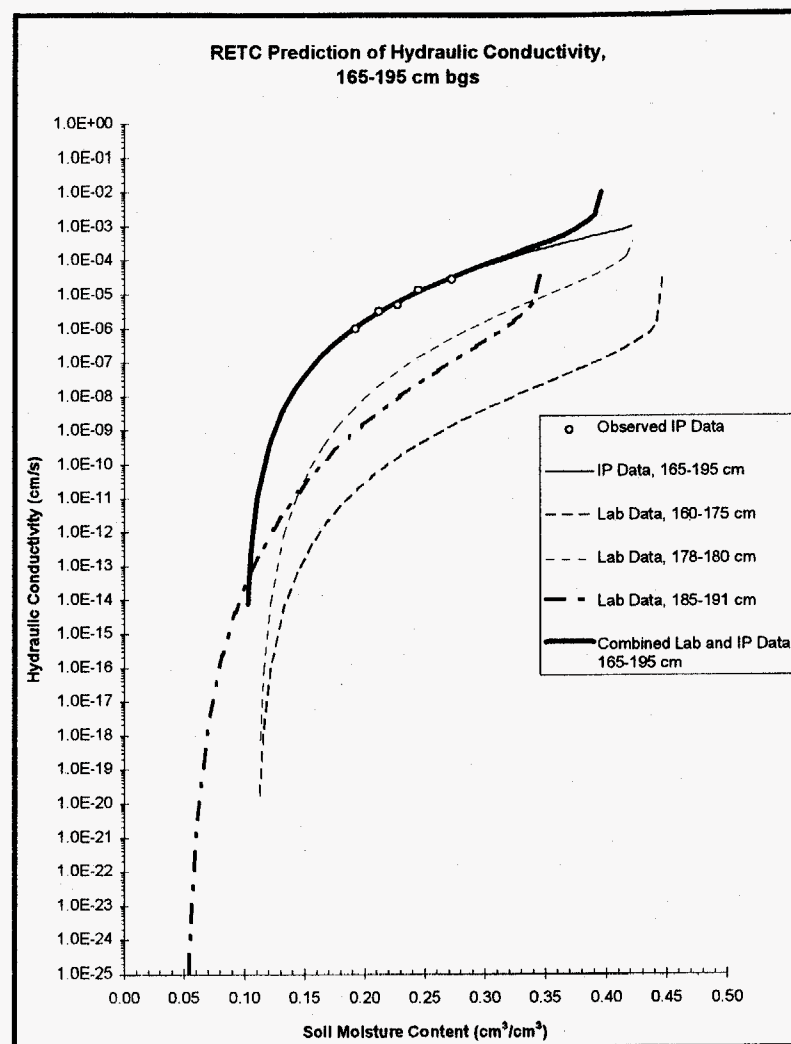


Figure A3-6. RETC-predicted $K(\theta)$ relationships from IP, laboratory, and combined laboratory and IP data, 165 - 195 cm bgs.

Distribution:

- 1 David Peterson
INTERA, Inc.
1650 University Blvd.
Albuquerque, NM 87102

- 1 MS 0720 R.G. Knowlton, 6603
- 1 1126 H.A. Nyugen, 7584
- 1 1126 C.S. Roepke, 7584
- 1 1126 W.R. Strong, 7584
- 1 1148 R.E. Fate, 7585
- 1 1148 T.J. Goering, 7585
- 1 1148 E.A. Klavetter, 7585
- 1 1148 M.D. McVey, 7585
- 1 1148 J.L. Peace, 7585

- 4 0184 J.O. Johnsen, DOE/KAO
- 1 1309 Environmental Operations Records Center, 7512

- 1 9018 Central Technical Files, 8523-2
- 5 0899 Technical Library, 4414
- 2 0619 Review & Approval Desk, 12630
For DOE/OSTI

